

# Random Forest Weighted Local Fréchet Regression

Rui Qiu and Zhou Yu

School of Statistics, East China Normal University

Ruoqing Zhu

Department of Statistics, University of Illinois at Urbana-Champaign

February 7, 2023

## Abstract

Statistical analysis is increasingly confronted with complex data from metric spaces. Petersen and Müller (2019) established a general paradigm of Fréchet regression with complex metric space valued responses and Euclidean predictors. However, the local approach therein involves nonparametric kernel smoothing and suffers from the curse of dimensionality. To address this issue, we in this paper propose a novel random forest weighted local Fréchet regression paradigm. The main mechanism of our approach relies on a locally adaptive kernel generated by random forests. Our first method utilizes these weights as the local average to solve the conditional Fréchet mean, while the second method performs local linear Fréchet regression, both significantly improving existing Fréchet regression methods. Based on the theory of infinite order U-processes and infinite order  $M_{m_n}$ -estimator, we establish the consistency, rate of convergence, and asymptotic normality for our local constant estimator, which covers the current large sample theory of random forests with Euclidean responses as a special case. Numerical studies show the superiority of our methods with several commonly encountered types of responses such as distribution functions, symmetric positive-definite matrices, and sphere data. The practical merits of our proposals are also demonstrated through the application to human mortality distribution data.

**Keyword:**Fréchet regression; Metric space; Random forest; Nonparametric regression; Mortality distribution

## 1 Introduction

In recent years, non-Euclidean statistical analysis has received increasing attention due to demands from modern applications, such as the covariance or correlation matrices for the functional brain connectivity in neuroscience and probability distributions in CT hematoma density data. To this end, Hein (2009) proposed nonparametric Nadaraya-Watson estimators for response variables being random objects, which are random elements in general metric spaces that by default do not have a vector space structure. Petersen and Müller (2019) further introduced the general framework of Fréchet regression and established the methodology and theory for both global and local Fréchet regression analysis of complex random objects. Chen and Müller (2022) continued to derive the uniform convergence rate of local Fréchet regression. Yuan et al. (2012) and Lin et al. (2022) considered nonparametric modeling with responses being symmetric positive-definite matrices, which are a specific type of random object. These methods certainly build a concrete foundation of statistical modeling with non-Euclidean responses. However, methods mentioned above rely on nonparametric kernel smoothing and thus can be problematic when the dimension of predictor  $X$  is relatively high, limiting the scope of Fréchet regression in real applications (Bhattacharjee and Müller, 2021; Ying and Yu, 2022; Zhang et al., 2021).

Random forest, as pioneered by Leo Breiman (Breiman, 2001), is a popular and promising tool for high dimensional statistical learning for Euclidean data. It is an ensemble model that combines the strength of multiple randomized trees. Random forests demonstrate substantial gains in regression and classification tasks compared to classical statistical methods. Moreover, the trees can be generated parallelly, making random forests more attractive computationally. Theoretical research into random forests has gained considerable momentum in recent years due to their tremendous popularity. Biau et al. (2008) first proved the consistency of purely random forests for classification. For regression problems, Genuer (2012) and Arlot and Genuer (2014) further made a complete analysis of the variance and bias of purely random forests. Biau (2012) and Gao and Zhou (2020) established the consistency and convergence rate of the centered random forests for regression and classification, respectively. Duroux and Scornet (2018) provided the convergence rate of  $q$ -quantile random forests. In particular, Klusowski (2021) improved the rate of the median random forests. Scornet et al. (2015) proved the  $L^2$  consistency of Breiman's original random forests for the first time under the assumption of additive model structure. Menth and Hooker (2016) formulated random forests as infinite order incomplete U-statistics and studied their

asymptotic normality. [Wager and Athey \(2018\)](#) further established the central limit theorem for random forests based on honest tree construction.

However, most methodology developments, theoretical investigations, and real applications of random forests focus on classical Euclidean responses and predictors. It is then of great interest to generalize the random forests with metric space valued responses, which is expected to work better than existing Fréchet regression methods when the predictor dimension is moderately large. To this end, [Capitaine et al. \(2019\)](#) proposed Fréchet trees and Fréchet random forests based on regression trees and Breiman's random forests. On the other hand, recent developments ([Lin and Jeon, 2006](#); [Meinshausen and Ridgeway, 2006](#); [Bloniarz et al., 2016](#); [Athey et al., 2019](#); [Friedberg et al., 2020](#)) reveal the fact that random forests implicitly construct a kernel-type weighting function. This proliferation of work points toward a general synthesis between the core of nonparametric kernel smoothing and the ability to encompass locally data-adaptive weighting by random forests. Taking a step forward, we in this paper propose a novel random forest weighted local Fréchet regression paradigm with superior performance and desirable statistical properties.

Our major contributions are summarized from the following three perspectives. First, to the best of our knowledge, this is the first attempt to adopt random forests as a kernel for Fréchet regression. Our proposal called random forest weighted local constant Fréchet regression articulates a new formulation of Fréchet regression based on random forests that has an intrinsic relationship with classical nonparametric kernel regression. Second, compared to [Capitaine et al. \(2019\)](#), our method is more concise in terms of formulation, which allows us to take a substantial step towards the asymptotic theory of local Fréchet regression based on random forests rigorously. Following the line of research introduced by [Wager and Athey \(2018\)](#) based on trees with honest and other properties, the consistency and rate of convergence are derived based on the theory of infinite order  $U$ -statistics and  $U$ -processes. To study the asymptotic normality, we extend the current theory of finite order  $M_m$ -estimator to infinite order  $M_{m_n}$ -estimator. The new technical tools developed to establish the central limit theorem of infinite order  $M_{m_n}$ -estimator can be of independent interest. And our asymptotic normality result also covers that of random forests with Euclidean responses ([Wager and Athey, 2018](#)) as a special case. Last but not least, the perspective from which we view the random forests facilitates the generalization of our method to the local linear version. This extension achieves better smoothness of the resulting estimator. The random forest weighted local constant Fréchet regression and local linear Fréchet regression collectively make up a coherent system and a new framework for Fréchet regression.

The rest of the paper is organized as follows. In Section 2, we give an overview of Fréchet regression and introduce the random forest weighted local constant Fréchet regression (RFWLCFR) method. In Section 3, we establish the consistency and develop the asymptotic convergence rate and asymptotic normality of RFWLCFR. In Section 4, we present the random forest weighted local linear Fréchet regression (RFWLLFR) approach as the generalization of RFWLCFR and confirm its consistency in estimation. In Section 5, we conduct comprehensive simulation studies to examine our proposals in different settings, including probability distributions, symmetric positive-definite matrices, and spherical data. In Section 6, we apply our methods to the Human Mortality Data, where the responses are age-at-death distributions. Section 7 concludes the paper with some discussions.

## 2 Proposed method

### 2.1 Fréchet regression

Let  $(\Omega, d)$  be a metric space equipped with a specific metric  $d$ . Let  $\mathcal{R}^p$  be the  $p$ -dimensional Euclidean space. We consider a random pair  $(X, Y) \sim F$ , where  $X \in \mathcal{R}^p$ ,  $Y \in \Omega$  and  $F$  is the joint distribution of  $(X, Y)$ . We denote the marginal distributions of  $X$  and  $Y$  as  $F_X$  and  $F_Y$ , respectively. The conditional distributions  $F_{X|Y}$  and  $F_{Y|X}$  are also assumed to exist. When  $\Omega = \mathcal{R}$ , the target of classical regression is the conditional mean

$$m(x) = E(Y \mid X = x) = \operatorname{argmin}_{y \in \mathcal{R}} E\{(Y - y)^2 \mid X = x\}.$$

Replacing the Euclidean distance with the intrinsic metric  $d$  of  $\Omega$ , conditional Fréchet mean ([Petersen and Müller, 2019](#)) can then be defined as

$$m_{\oplus}(x) = \operatorname{argmin}_{y \in \Omega} M_{\oplus}(x, y) = \operatorname{argmin}_{y \in \Omega} E\{d^2(Y, y) \mid X = x\}. \quad (1)$$

Given an i.i.d training sample  $\mathcal{D}_n = \{(X_1, Y_1), \dots, (X_n, Y_n)\}$  with  $(X_i, Y_i) \sim F$ , the goal of Fréchet regression is to estimate  $m_{\oplus}(x)$  in the sample level. For this purpose, [Hein \(2009\)](#) generalized the Nadaraya-Watson regression to the Fréchet version as

$$\hat{m}_{\oplus}^{\text{NW}}(x) = \operatorname{argmin}_{y \in \Omega} \frac{1}{n} \sum_{i=1}^n K_h(X_i - x) d^2(Y_i, y),$$

where  $K$  is a smoothing kernel such as the Epanechnikov kernel or Gaussian Kernel and  $h$  is a bandwidth, with  $K_h(\cdot) = h^{-1}K(\cdot/h)$ . [Petersen and Müller \(2019\)](#) recharacterized the standard multiple linear regression and local linear regression as a function of weighted Fréchet means, and proposed global Fréchet regression and local Fréchet regression as

$$\hat{m}_\oplus(x) = \operatorname{argmin}_{y \in \Omega} \frac{1}{n} \sum_{i=1}^n s_{in}(x) d^2(Y_i, y),$$

where  $s_{in}(x)$  has different expressions for global and local Fréchet regression.

The Nadaraya-Watson Fréchet regression and local Fréchet regression both involve kernel weighting function  $K$  in the estimation procedure, which limits their applications when  $p \geq 3$ . To address this issue, we borrow the strength of random forests to generate a more powerful weighting function for moderately large  $p$ .

## 2.2 Local constant method

The prediction error of the random forest is related to the number of trees and the correlation among different trees. In addition to resampling the training data set for the growing of individual trees, auxiliary randomness is often introduced to further reduce the correlation between trees and improve the prediction accuracy of random forests. For example, a subset of features is randomly selected before each split, and the split direction is designed based on the subset only. Here, we denote  $\xi \sim \Xi$  as a source of auxiliary randomness.

We first consider the classical random forests with Euclidean responses ( $\Omega = \mathcal{R}$ ). And each tree is trained on a subsample  $\mathcal{D}_n^b = \{(X_{i_{b,1}}, Y_{i_{b,1}}), (X_{i_{b,2}}, Y_{i_{b,2}}), \dots, (X_{i_{b,s_n}}, Y_{i_{b,s_n}})\}$  of the training data set  $\mathcal{D}_n$ , with  $1 \leq i_{b,1} < i_{b,2} < \dots < i_{b,s_n} \leq n$ . Throughout the paper, we assume that the subsample size  $s_n \rightarrow +\infty$  and  $s_n/n \rightarrow 0$  as  $n$  tends to infinity. Data resampling is done here without replacement (see [Scornet et al. \(2015\)](#); [Morch and Hooker \(2016\)](#); [Wager and Athey \(2018\)](#)). The  $b$ th tree  $T_b$  constructed by  $\mathcal{D}_n^b$  and a random draw  $\xi_b \sim \Xi$  gives an estimator of  $m(x)$

$$T_b(x; \mathcal{D}_n^b, \xi_b) = \frac{1}{N(L_b(x; \mathcal{D}_n^b, \xi_b))} \sum_{i: X_i \in L_b(x; \mathcal{D}_n^b, \xi_b)} Y_i,$$

where  $N(L_b(x; \mathcal{D}_n^b, \xi_b))$  is the number of samples in  $L_b(x; \mathcal{D}_n^b, \xi_b)$ , the leaf node containing  $x$  of  $T_b$ . For the random forest constructed based on a total number of  $B$  randomized regression trees, the estimator of  $m(x)$  becomes

$$\text{RF}(x) = \frac{1}{B} \sum_{b=1}^B T_b(x; \mathcal{D}_n^b, \xi_b) = \frac{1}{B} \sum_{b=1}^B \frac{1}{N(L_b(x; \mathcal{D}_n^b, \xi_b))} \sum_{i: X_i \in L_b(x; \mathcal{D}_n^b, \xi_b)} Y_i.$$

In fact, we can also regard it as a weighted average of the training responses,

$$\text{RF}(x) = \sum_{i=1}^n \alpha_i(x) Y_i, \tag{2}$$

where  $\alpha_i(x) = \frac{1}{B} \sum_{b=1}^B \frac{1_{\{X_i \in L_b(x; \mathcal{D}_n^b, \xi_b)\}}}{N(L_b(x; \mathcal{D}_n^b, \xi_b))}$  is defined as the random forest kernel.

To generalize the Euclidean random forests when  $\Omega$  is a general metric space, we rewrite the random forest estimator (13) as the implicit minimizer of certain objective function

$$\text{RF}(x) = \operatorname{argmin}_{y \in \mathcal{R}} \sum_{i=1}^n \alpha_i(x) (Y_i - y)^2.$$

By simply replacing the Euclidean distance by the metric  $d$  of  $\Omega$ , we get

$$\text{RF}_\oplus(x) = \operatorname{argmin}_{y \in \Omega} \sum_{i=1}^n \alpha_i(x) d^2(Y_i, y). \tag{3}$$

In the generalization (15), random forests produce the weighting function  $\alpha_i(x)$  for Fréchet regression but do not participate in the prediction. It should be noted that the random forest here is constructed by Fréchet trees, which are regression trees with metric space valued responses regardless of their split criterion. Since (15) is essentially a local constant estimator based on the random forest kernel, we call it random forest weighted local constant Fréchet regression. Our proposal is expected to outperform Nadaraya-Watson Fréchet regression estimator ([Hein, 2009](#)) and the local Fréchet regression estimator ([Petersen and Müller, 2019](#)) for the following two reasons. Firstly, the random forest kernel can handle moderately large  $p$ . Secondly, if the split criterion of Fréchet trees depends on the response  $Y$ , the random forest kernel will be adaptive in the sense that it incorporates both the information of  $X$  and  $Y$ . Here we use a simulation example to illustrate the adaptiveness of random forest kernel based on 100 Fréchet trees with the variance reduction splitting criterion introduced in section A.1 of appendix.

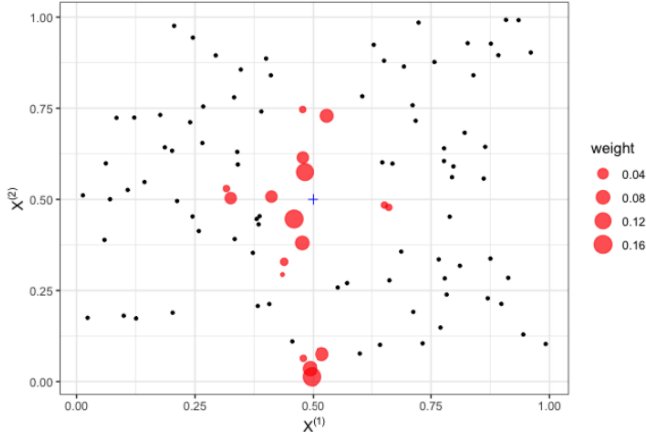


Figure 1: Weights given by the random forest kernel. Each circle represents a training sample point. The red circles represent points whose weights to  $(0.5, 0.5)$  are greater than 0 and diameter of these circles indicates the size of weights.

**Example 1.** Consider a Fréchet regression problem for a distribution-valued response  $Y$  with a predictor  $X = (X^{(1)}, X^{(2)}) \sim \mathcal{U}([0, 1]^2)$  as

$$Y = N\left(X^{(1)} \sin(4X^{(1)}\pi) + \epsilon, 1\right), \quad (4)$$

where  $\epsilon \sim \mathcal{N}(0, 0.2^2)$ . The values of the random forest kernel at 100 training sample points when making a prediction at the center  $(0.5, 0.5)$  are displayed in Fig. 1. It can be observed that the weights decay much more quickly along the  $X^{(1)}$  direction and are less influenced by the value of  $X^{(2)}$ . Under the construction mechanism of the random forest, samples that are close to the target point in the  $X^{(1)}$  direction are considered important for prediction, which is consistent with the fact that  $Y$  is only relevant to  $X^{(1)}$  in (4). Unlike the random forest kernel, the Euclidean distance based kernel does not have such an adaptive nature, and the local neighborhoods for the target point do not spread out in the flat directions.

### 3 Theoretical properties

#### 3.1 Population target

This section is devoted to the asymptotic analysis of random forest weighted local constant Fréchet regression. Here we consider a random pair  $(X, Y) \sim F$ , where  $X$  and  $Y$  take values in  $[0, 1]^p$  and  $\Omega$ . To facilitate further theoretical investigations, we follow [Wager and Athey \(2018\)](#) and assume that  $B \rightarrow \infty$  given infinite computing power. Let  $\bar{\alpha}_i(x) = \lim_{B \rightarrow \infty} \alpha_i(x) = \lim_{B \rightarrow \infty} \frac{1}{B} \sum_{b=1}^B \frac{1\{X_i \in L_b(x; \mathcal{D}_n^b, \xi_b)\}}{N(L_b(x; \mathcal{D}_n^b, \xi_b))}$ . Instead of studying the  $\text{RF}_\oplus(x)$  defined in (15), we consider the infinite forest version

$$\hat{r}_\oplus(x) = \underset{y \in \Omega}{\text{argmin}} \hat{R}_n(x, y) = \underset{y \in \Omega}{\text{argmin}} \sum_{i=1}^n \bar{\alpha}_i(x) d^2(Y_i, y), \quad (5)$$

and develop the corresponding large sample theory. The assumption that  $B$  is large enough for Monte Carlo effects not to matter is inspired by [Scornet et al. \(2015\)](#), [Wager and Athey \(2018\)](#) and many other works. In practice we can choose  $B$  as large as possible. We see

$$\begin{aligned} \hat{r}_\oplus(x) &= \underset{y \in \Omega}{\text{argmin}} \sum_{i=1}^n \left[ \lim_{B \rightarrow \infty} \frac{1}{B} \sum_{b=1}^B \frac{1\{X_i \in L_b(x; \mathcal{D}_n^b, \xi_b)\}}{N(L_b(x; \mathcal{D}_n^b, \xi_b))} \right] d^2(Y_i, y) \\ &= \underset{y \in \Omega}{\text{argmin}} \lim_{B \rightarrow \infty} \frac{1}{B} \sum_{b=1}^B \left\{ \frac{1}{N(L_b(x; \mathcal{D}_n^b, \xi_b))} \sum_{i: X_i \in L_b(x; \mathcal{D}_n^b, \xi_b)} d^2(Y_i, y) \right\} \\ &= \underset{y \in \Omega}{\text{argmin}} \left( \binom{n}{s_n} \right)^{-1} \sum_k E_{\xi \sim \Xi} \left\{ \frac{1}{N(L(x; \mathcal{D}_n^k, \xi))} \sum_{i: X_i \in L(x; \mathcal{D}_n^k, \xi)} d^2(Y_i, y) \right\}, \end{aligned} \quad (6)$$

where the summation about  $k$  is taken over all  $\binom{n}{s_n}$  subsamples of size  $s_n$ ,  $\mathcal{D}_n^k$  is the  $k$ th subsample of  $\mathcal{D}_n$ , and the expectation is taken about the random effect  $\xi$ .  $B \rightarrow \infty$  is equivalent to considering all subsamples of  $\mathcal{D}_n$  and all  $\xi$

conditioned on each subsample, which implies (6). As  $s_n \rightarrow \infty$  when  $n \rightarrow \infty$ , the objective function  $\hat{R}_n(x, y)$  of  $\hat{r}_\oplus(x)$  is an infinite order U-statistic with rank  $s_n$  for any fixed  $y \in \Omega$ .

Based on (5) and (6), we define two population level versions of  $\hat{r}_\oplus(x)$  as follows.

$$\begin{aligned}\tilde{r}_\oplus(x) &= \operatorname{argmin}_{y \in \Omega} \tilde{R}_n(x, y) = \operatorname{argmin}_{y \in \Omega} nE\{\bar{\alpha}_i(x) d^2(Y_i, y)\} \\ &= \operatorname{argmin}_{y \in \Omega} E\left\{\frac{1}{N(L(x; \mathcal{D}_n^k, \xi))} \sum_{i: X_i \in L(x; \mathcal{D}_n^k, \xi)} d^2(Y_i, y)\right\},\end{aligned}\quad (7)$$

where the expectation is taken about all randomness. We separate  $d(\hat{r}_\oplus(x), m_\oplus(x))$  into the bias term  $d(\tilde{r}_\oplus(x), m_\oplus(x))$  and the variance term  $d(\hat{r}_\oplus(x), \tilde{r}_\oplus(x))$  for asymptotic analysis.

### 3.2 Consistency

To study the consistency of  $\hat{r}_\oplus(x)$ , we assume the following regularity conditions.

(A1)  $(\Omega, d)$  is a bounded metric space, i.e.,  $\operatorname{diam}(\Omega) = \sup_{y_1, y_2 \in \Omega} d(y_1, y_2) < \infty$ .

(A2) The marginal density  $f$  of  $X$ , as well as the conditional densities  $g_y$  of  $X \mid Y = y$ , exist and are bounded and continuous, the latter for all  $y \in \Omega$ . And  $f$  is also bounded away from zero such that  $0 < f_{\min} \leq f$ . Additionally, for any open  $V \subset \Omega$ ,  $\int_V dF_{Y|X}(x, y)$  is continuous as a function of  $x$ .

(A3)  $\operatorname{diam}(L(x)) \rightarrow 0$  in probability, where  $L(x)$  is the leaf node containing  $x$  of any Fréchet tree involved in the generation of the random forest kernel  $\bar{\alpha}_i(x)$ .

(A4) The object  $m_\oplus(x)$  exists and is unique. For all  $n$ ,  $\tilde{r}_\oplus(x)$  and  $\hat{r}_\oplus(x)$  exist and are unique, the latter almost surely. Additionally, for any  $\varepsilon > 0$ ,

$$\begin{aligned}\inf_{d(y, m_\oplus(x)) > \varepsilon} \{M_\oplus(x, y) - M_\oplus(x, m_\oplus(x))\} &> 0, \\ \liminf_n \inf_{d(y, \tilde{r}_\oplus(x)) > \varepsilon} \{\tilde{R}_n(x, y) - \tilde{R}_n(x, \tilde{r}_\oplus(x))\} &> 0.\end{aligned}$$

Assumptions (A1), (A2) and (A4) are commonly used conditions to study the Fréchet regression, see [Petersen and Müller \(2019\)](#). If the termination condition for the growth of each Fréchet tree is that the number of samples in the leaf nodes does not exceed a certain constant, for example, the Fréchet tree is  $\alpha$ -regular, which will be mentioned in section 3.3, the assumption (A3) will hold (see Lemma 2 of [Wager and Athey \(2018\)](#)). Similar conditions can also be found in [Denil et al. \(2013\)](#). The assumption (A4) is also a regular condition to guarantee the consistency of M-estimator (see Corollary 3.2.3 of [van der Vaart and Wellner \(1996\)](#)). The simulation in section 5 will consider three kinds of metric spaces: probability distributions equipped with the Wasserstein metric, symmetric positive definite matrices equipped with Log-Cholesky metric or the affine-invariant metric and unit sphere equipped with geodesic distance. The first two can satisfy the assumption (A4) naturally or under very weak conditions. For the last one, uniqueness of Fréchet means is generally not guaranteed, but can be satisfied under certain circumstances, for example restricting the support of the underlying distribution.

In addition to assumptions (A1)–(A4), we further require that Fréchet trees are constructed with honesty and symmetry as defined in [Wager and Athey \(2018\)](#). More instructions about honesty are given in the appendix and can easily be adapted to Fréchet trees.

(a) (*Honest*) The Fréchet tree is honest if the training examples whose responses have been used to decide where to place the splits can not be involved in the calculation of the random forest kernel.

(b) (*Symmetric*) The Fréchet tree is symmetric if the output of the tree does not depend on the order ( $i = 1, 2, \dots$ ) in which the training examples are indexed.

**Theorem 1.** Suppose that for a fix  $x \in [0, 1]^p$ , (A1)–(A4) hold and Fréchet trees are honest and symmetric. Then  $\hat{r}_\oplus(x)$  is pointwise consistent, i.e.,

$$d(\hat{r}_\oplus(x), m_\oplus(x)) = o_p(1).$$

**Remark 1.** Building infinite Fréchet trees is actually computationally intensive. In fact, the above results also hold true with  $B = B_n < \binom{n}{s_n}$  where  $B_n \rightarrow \infty$  as  $n \rightarrow \infty$ . Consider

$$\hat{r}_\oplus(x) = \operatorname{argmin}_{y \in \Omega} \hat{R}_n(x, y) = \operatorname{argmin}_{y \in \Omega} \frac{1}{B_n} \sum_{b=1}^{B_n} \left\{ \frac{1}{N(L_b(x; \mathcal{D}_n^b, \xi_b))} \sum_{i: X_i \in L_b(x; \mathcal{D}_n^b, \xi_b)} d^2(Y_i, y) \right\}.$$

In this case,  $\hat{R}_n(x, y)$  is called an incomplete infinite order U-statistic with random kernel (about  $\xi_b$ ) for each fixed  $y \in \Omega$ , which in general does not fit within the framework of infinite order U-statistics. But the randomization parameter  $\xi \sim \Xi$  is usually independent of the training sample  $\mathcal{D}_n$ . The consistency of  $\hat{R}_n(x, y) - \tilde{R}_n(x, y) = o_p(1)$  for each  $y \in \Omega$  still holds. Then by the same proof as Theorem 1,  $\hat{r}_\oplus(x)$  is still pointwise consistent with finite Fréchet trees. But the tool of incomplete infinite order U-processes with random kernel is not clear so far. So the convergence rate and asymptotic normality in the section 3.3, 3.4 will still be developed under the constraint  $B \rightarrow \infty$ .

If the previous assumptions are suitably strengthened, we can further obtain the uniform convergence results for  $\hat{r}_\oplus(x)$ . Let  $\|\cdot\|$  be the Euclidean norm on  $\mathcal{R}^p$  and  $J > 0$ .

(U1) For any  $\|x\| \leq J$ ,  $M_\oplus(x, y)$  is equicontinuous, i.e.,

$$\limsup_{\dot{x} \rightarrow x} \sup_{y \in \Omega} |M_\oplus(\dot{x}, y) - M_\oplus(x, y)| = 0.$$

(U2) The marginal density  $f$  of  $X$ , as well as the conditional densities  $g_y$  of  $X \mid Y = y$ , exist and are bounded and uniformly continuous, the latter for all  $y \in \Omega$ . And  $f$  is also bounded away from zero such that  $0 < f_{\min} \leq f$ . Additionally, for any open  $V \subset \Omega$ ,  $\int_V dF_{Y|X}(x, y)$  is continuous as a function of  $x$ .

(U3)  $\sup_{\|x\| \leq J} \text{diam}(L(x)) \rightarrow 0$  in probability, where  $L(x)$  is the leaf node containing  $x$  of any Fréchet tree involved in the generation of the random forest kernel  $\bar{a}_i(x)$ .

(U4) For all  $\|x\| \leq J$ ,  $m_\oplus(x)$ ,  $\tilde{r}_\oplus(x)$  and  $\hat{r}_\oplus(x)$  exist and are unique, the latter almost surely. Additionally, for any  $\varepsilon > 0$ ,

$$\inf_{\|x\| \leq J} \inf_{d(y, m_\oplus(x)) > \varepsilon} \{M_\oplus(x, y) - M_\oplus(x, m_\oplus(x))\} > 0,$$

$$\liminf_n \inf_{\|x\| \leq J} \inf_{d(y, \hat{r}_\oplus(x)) > \varepsilon} \left\{ \tilde{R}_n(x, y) - \tilde{R}_n(x, \hat{r}_\oplus(x)) \right\} > 0,$$

and there exists  $\zeta = \zeta(\varepsilon) > 0$  such that

$$P \left\{ \inf_{\|x\| \leq J} \inf_{d(y, \hat{r}_\oplus(x)) > \varepsilon} \left( \hat{R}_n(x, y) - \hat{R}_n(x, \hat{r}_\oplus(x)) \right) \geq \zeta \right\} \rightarrow 1.$$

**Theorem 2.** Suppose that (A1), (U1)–(U4) hold and Fréchet trees are honest and symmetric. Then

$$\sup_{\|x\| \leq J} d(\hat{r}_\oplus(x), m_\oplus(x)) = o_p(1).$$

### 3.3 Rate of Convergence

To bound the bias term and further eliminate the bias when deriving the asymptotic normality, we follow [Wager and Athey \(2018\)](#) to place the following additional requirements on the construction of Fréchet trees.

(c) (*Random-split*) At each node split, marginalizing over  $\xi$ , the probability that  $X_j (1 \leq j \leq p)$  is selected as the split variable is bounded below by  $\pi/p$  for some  $0 < \pi \leq 1$ .

(d) ( *$\alpha$ -regular*) After each splitting, each child node contains at least a fraction  $\alpha > 0$  of the available training sample. Moreover, the tree stops to grow if every leaf node contains only between  $k$  and  $2k - 1$  observations, where  $k$  is some fixed integer.

To derive convergence rate, some additional assumptions are required. We start with some notations. Let  $Z_i = (X_i, Y_i)$  and  $\mathcal{D}_n^k = (Z_{i_{k,1}}, Z_{i_{k,2}}, \dots, Z_{i_{k,s_n}})$ , and define

$$H_n(Z_{i_{k,1}}, \dots, Z_{i_{k,s_n}}, y) = E_{\xi \sim \Xi} \left[ \frac{1}{N(L(x; \mathcal{D}_n^k, \xi))} \sum_{i: X_i \in L(x; \mathcal{D}_n^k, \xi)} \{d^2(Y_i, y) - d^2(Y_i, \tilde{r}_\oplus(x))\} \right].$$

Consider the function class

$$\mathcal{H}_\delta := \{H_n(z_1, \dots, z_{s_n}, y) : d(y, \tilde{r}_\oplus(x)) < \delta\}.$$

Let  $Z_i^0 = (X_i, Y_i)$ , for  $i = 1, \dots, n$ , and let  $\{Z_i^1\}_{i=1}^n$  be i.i.d., independent of  $\{Z_i^0\}_{i=1}^n$  with the same distribution. For  $\forall H_n(y_1), H_n(y_2) \in \mathcal{H}_\delta$ , define the following random pseudometric

$$d_j(H_n(y_1), H_n(y_2)) = \frac{\sum_{k=1}^n \left| \sum_{a \in (n)_{s_n}: a_1=k} H_n(Z_{a_j}^{0,1}; y_1) - H_n(Z_{a_j}^{0,1}; y_2) \right|}{\sum_{a \in (n)_{s_n}} G_\delta(Z_{a_j}^{0,1})},$$

where  $Z_{a_j}^{0,1} = (Z_{a_1}^0, \dots, Z_{a_j}^0, Z_{a_{j+1}}^1, \dots, Z_{a_{s_n}}^1)$ ,  $(n)_{s_n}$  represents all the permutations of taking  $s_n$  distinct elements from the set  $\{1, 2, \dots, n\}$ , and  $G_\delta$  is an envelope function for  $\mathcal{H}_\delta$  such that  $|H_n| \leq G_\delta$  for every  $H_n \in \mathcal{H}_\delta$ .

With the above preparation, the assumptions are specified as follows.

(A5) For each  $y$ ,  $M_\oplus(x, y)$  is Lipschitz-continuous about  $x$ , and the Lipschitz constant has a common upper bound  $K$ .

(A6) There exist  $\delta_1 > 0$ ,  $C_1 > 0$  and  $\beta_1 > 1$ , possibly depending on  $x$ , such that, whenever  $d(y, m_\oplus(x)) < \delta_1$ , we have  $M_\oplus(x, y) - M_\oplus(x, m_\oplus(x)) \geq C_1 d(y, m_\oplus(x))^{\beta_1}$ .

(A7) There exist constants  $A$  and  $V$  such that

$$\max_{j \leq s_n} N(\varepsilon, d_j, \mathcal{H}_\delta) \leq A \varepsilon^{-V}$$

as  $\delta \rightarrow 0$  for any  $\epsilon \in (0, 1]$ , where  $N(\epsilon, d_j, \mathcal{H}_\delta)$  is the  $\epsilon$ -covering number of the function class  $\mathcal{H}_\delta$  based on the pseudometric  $d_j$  we introduce.

(A8) There exist  $\delta_2 > 0, C_2 > 0$  and  $\beta_2 > 1$ , possibly depending on  $x$ , such that, whenever  $d(y, \tilde{r}_\oplus(x)) < \delta_2$ , we have

$$\liminf_n \left\{ \tilde{R}_n(x, y) - \tilde{R}_n(x, \tilde{r}_\oplus(x)) - C_2 d(y, \tilde{r}_\oplus(x))^{\beta_2} \right\} \geq 0.$$

The Lipschitz continuity in the assumption (A5) allows us to control the bias term by restricting the diameter of the sample space represented by the leaf node. The assumption (A7) along with the pseudometric  $d_j$  were proposed by Heilig (1997) and Heilig and Nolan (2001) to establish the maximal inequality of infinite order U-processes. From the perspective of empirical process, (A7) regulates  $\mathcal{H}_\delta$  a Euclidean class. Knowing that a class of functions is Euclidean aids immensely in establishing the convergence rate of the variance term. The assumptions (A6) and (A8) comes from Petersen and Müller (2019). (A8) is also an extension of the condition that controls the convergence rate of  $M$ -estimator. Please refer to Theorem 3.2.5 of van der Vaart and Wellner (1996) for more details.

**Theorem 3.** Suppose that for a fixed  $x \in [0, 1]^p$ , (A1), (A2), (A4)–(A8) hold, and Fréchet trees are  $\alpha$ -regular, random-split, honest and symmetric. If  $\alpha \leq 0.2$ , then

$$d(\hat{r}_\oplus(x), m_\oplus(x)) = O_p \left( s_n^{-\frac{1}{2} \frac{\log((1-\alpha)^{-1})}{\log(\alpha^{-1})} \frac{1}{p} \frac{1}{\beta_1-1}} + \left( \frac{s_n^2 \log s_n}{n} \right)^{\frac{1}{2(\beta_2-1)}} \right).$$

### 3.4 Asymptotic Normality

There are two major difficulties in deriving the asymptotic normality of our proposed  $\hat{r}_\oplus(x)$ . On the one hand, it is not the classical  $M$ -estimator, but  $M_m$ -estimator (Bose and Chatterjee, 2018) and even  $M_{m_n}$ -estimator with infinite order U-processes. So we have to deal with the most general  $M_{m_n}$ -estimator, where  $m_n$  diverges to infinity. On the other hand, the  $M_{m_n}$ -estimator here takes value not in Euclidean space but in general metric space, which will also bring difficulties to the study of asymptotic limiting distribution. To address the first difficulty, we will generalize the result in section 2.5 of Bose and Chatterjee (2018) to acquire the probability representation and asymptotic normality of the  $M_{m_n}$ -estimator. We put this content in the section C of appendix due to space limitations. As for the second issue, the seminal work of Bhattacharya and Lin (2017) and Bhattacharya and Patrangenaru (2003, 2005) concluded that the map of the sample Fréchet mean is asymptotically normally distributed around the map of the Fréchet mean under certain assumptions. We follow their developments in combination with our developed asymptotic tool for  $M_{m_n}$ -estimator to establish the asymptotic normality of  $\hat{r}_\oplus(x)$  finally. Here we continue to adopt the expressions (6) and (7). Let

$$h_n(Z_{i_{k,1}}, Z_{i_{k,2}}, \dots, Z_{i_{k,s_n}}, y) = E_{\xi \sim \Xi} \left\{ \frac{1}{N(L(x; \mathcal{D}_n^k, \xi))} \sum_{i: X_i \in L(x; \mathcal{D}_n^k, \xi)} d^2(Y_i, y) \right\}$$

where  $Z_i = (X_i, Y_i)$  and  $\mathcal{D}_n^k = (Z_{i_{k,1}}, Z_{i_{k,2}}, \dots, Z_{i_{k,s_n}})$ . Then

$$\hat{r}_\oplus(x) = \operatorname{argmin}_{y \in \Omega} \hat{R}_n(x, y) = \operatorname{argmin}_{y \in \Omega} \left( \frac{n}{s_n} \right)^{-1} \sum_{1 \leq i_1 < i_2 < \dots < i_{s_n} \leq n} h_n(Z_{i_1}, Z_{i_2}, \dots, Z_{i_{s_n}}, y),$$

$$\tilde{r}_\oplus(x) = \operatorname{argmin}_{y \in \Omega} \tilde{R}_n(x, y) = \operatorname{argmin}_{y \in \Omega} E h_n(Z_1, Z_2, \dots, Z_{s_n}, y).$$

Unfortunately, since  $y$  is not in the Euclidean space, the derivative about  $y$  can't be computed and  $\hat{r}_\oplus(x) - \tilde{r}_\oplus(x)$  has no sense. In order to apply the Theorem 6 in appendix, we consider mapping  $y$  to the Euclidean space locally and assume

(A9)  $h_n(z_1, z_2, \dots, z_{s_n}, y)$  is measurable in  $(z_1, z_2, \dots, z_{s_n})$  and  $\tilde{R}_n(x, y) < \infty$  for each  $y$  and  $n$ .

(A10)  $\tilde{r}_\oplus(x)$  exists and is unique for each  $n$ .

(A11)  $\tilde{r}_\oplus(x) \in G$  for large  $n$ , where  $G$  is a measurable subset of  $\Omega$ . And there is a homeomorphism  $\phi : G \rightarrow U$ , where  $U$  is an open subset of  $\mathcal{R}^d$  for some  $d \geq 1$ , and  $G$  is given its relative topology on  $\Omega$ . Also

$$u \mapsto f_n(z_1, z_2, \dots, z_{s_n}, u) = h_n(z_1, z_2, \dots, z_{s_n}, \phi^{-1}(u))$$

is twice differentiable on an appropriate neighborhood of  $\phi(\tilde{r}_\oplus(x))$ .

(A12)  $f_n(z_1, z_2, \dots, z_{s_n}, u)$  is convex in  $u$  for each  $n$ .

(A13) Let  $g_n$  be a measurable sub-gradient of  $f_n$  about  $u$ . Define

$$K_n = \operatorname{Var} \{ E [g_n(Z_1, Z_2, \dots, Z_{s_n}, \phi(\tilde{r}_\oplus(x))) \mid Z_1] \},$$

then  $E |g_n(Z_1, Z_2, \dots, Z_{s_n}, \phi(\tilde{r}_\oplus(x)))|^2 < \infty$  for each  $n$ , and  $s_n \lambda_{\min}(K_n) \rightarrow 0$ .

(A14)  $H_n = \nabla^2 E f_n(Z_1, Z_2, \dots, Z_{s_n}, \phi(\tilde{r}_\oplus(x)))$  exists and is positive definite for each  $n$ , and  $\lambda_{\min}(H_n) \rightarrow 0$ .

The assumption (A11) is crucial just like the assumption for establishing the asymptotic normality of sample Fréchet mean as suggested in Bhattacharya and Lin (2017). Other assumptions are adaptions of that of Theorem 6 in appendix.

**Theorem 4.** Suppose that for a fixed  $x \in [0, 1]^p$ , (A1), (A4), (A9)–(A14) hold, and the Fréchet trees are symmetric. Then  $\phi(\hat{r}_\oplus(x))$  is asymptotically normal, i.e.,

$$n^{1/2} \Lambda_n^{-1/2} \{ \phi(\hat{r}_\oplus(x)) - \phi(\tilde{r}_\oplus(x)) \} \rightarrow \mathcal{N}(0, I),$$

where  $\Lambda_n = s_n^2 H_n^{-1} K_n H_n^{-1}$ .

If the homeomorphism  $\phi$  in Theorem 4 is Lipschitz-continuous, we can further get the asymptotic normality of  $\phi(\hat{r}_\oplus(x))$  about  $\phi(m_\oplus(x))$ .

**Corollary 1.** Suppose that for a fixed  $x \in [0, 1]^p$ , (A1), (A2), (A4)–(A6) and (A9)–(A14) hold. And assume that the homeomorphism  $\phi$  is Lipschitz-continuous. Moreover, the Fréchet trees are  $\alpha$ -regular, random-split, honest and symmetric. Then if  $\alpha \leq 0.2$  and the subsample size  $s_n$  satisfies

$$s_n \asymp n^\beta \quad \text{for some} \quad \beta_{\min} := 1 - \left\{ 1 + \frac{p}{\pi} \frac{\log(\alpha^{-1}) (\beta_1 - 1)}{\log((1 - \alpha)^{-1})} \right\}^{-1} < \beta < 1,$$

we have

$$n^{1/2} \Lambda_n^{-1/2} \{ \phi(\hat{r}_\oplus(x)) - \phi(m_\oplus(x)) \} \rightarrow \mathcal{N}(0, I).$$

**Remark 2.** Consider the special case when  $\Omega$  is a bounded subset of  $\mathcal{R}$ . And we take  $\phi$  as the identity mapping and  $\beta_1 = 2$ . This mapping is naturally Lipschitz-continuous. By Corollary 1, when  $s_n \asymp n^\beta$  for some  $\beta_{\min} := 1 - \left\{ 1 + \frac{p}{\pi} \frac{\log(\alpha^{-1})}{\log((1 - \alpha)^{-1})} \right\}^{-1} < \beta < 1$ , we have

$$\frac{n^{1/2} \{ \hat{r}_\oplus(x) - m_\oplus(x) \}}{s_n \zeta_{1,n}^{1/2}} \rightarrow \mathcal{N}(0, 1),$$

where  $\zeta_{1,n} = \text{Var} \left\{ E \left[ E_{\xi \sim \Xi} \left( \frac{1}{N(L(x; \mathcal{D}_n^*, \xi))} \sum_{i: X_i \in L(x; \mathcal{D}_n^*, \xi)} Y_i \right) \mid Z_1 \right] \right\}$  with  $\mathcal{D}_n^* = (Z_1, \dots, Z_{s_n})$ . Here  $\hat{r}_\oplus(x)$  is exactly the prediction of Euclidean random forest at  $x$ . This result coincides with Theorem 1 of [Wager and Athey \(2018\)](#). Therefore, our asymptotic normality established for Fréchet regression with metric space valued responses includes their result for Euclidean random forests as a special case.

## 4 Local Linear Smoothing

In section 2, we have proposed random forest weighted local constant Fréchet regression, which is a Nadaraya-Watson type estimator using random forest kernel. A very natural extension is to carry out local linear Fréchet regression further. The local linear estimator is more flexible and accurate in capturing smooth signals. Local Fréchet regression proposed by [Petersen and Müller \(2019\)](#) is a novel local linear estimator adapted to cases with metric space valued responses. Similar to the classical local linear estimator, their method still suffers from the curse of dimensionality. This section proposes the second method called random forest weighted local linear Fréchet regression, which adopts the random forest kernel to local linear Fréchet regression.

[Bloniarz et al. \(2016\)](#) and [Friedberg et al. \(2020\)](#) considered a local linear regression with Euclidean responses based on the random forest kernel

$$(\hat{\beta}_0, \hat{\beta}_1) = \underset{\beta_0, \beta_1}{\text{argmin}} \frac{1}{n} \sum_{i=1}^n \alpha_i(x) \{ Y_i - \beta_0 - \beta_1^T (X_i - x) \}^2, \quad (8)$$

where  $\alpha_i(x) = \frac{1}{B} \sum_{b=1}^B \frac{1 \{ X_i \in L_b(x; \mathcal{D}_n^b, \xi_b) \}}{N(L_b(x; \mathcal{D}_n^b, \xi_b))}$ . Then define the random forest weighted local linear estimator as

$$\hat{l}(x) = \hat{\beta}_0 = e_1^T (\tilde{X}^T A \tilde{X})^{-1} \sum_{i=1}^n \begin{pmatrix} 1 \\ X_i - x \end{pmatrix} \alpha_i(x) Y_i \quad (9)$$

where

$$\tilde{X} := \begin{pmatrix} 1 & X_{11} - x_1 & \dots & X_{1p} - x_p \\ 1 & X_{21} - x_1 & \dots & X_{2p} - x_p \\ \vdots & \vdots & \ddots & \vdots \\ 1 & X_{n1} - x_1 & \dots & X_{np} - x_p \end{pmatrix}, A := \text{diag}(\alpha_1(x), \dots, \alpha_n(x)), e_1 := \begin{pmatrix} 1 \\ 0 \\ \vdots \\ 0 \end{pmatrix}.$$

To generalize (9) with metric space valued responses, we rewrite it as an implicit form

$$\hat{l}(x) = \operatorname{argmin}_{y \in \mathcal{R}} e_1^T (\tilde{X}^T A \tilde{X})^{-1} \sum_{i=1}^n \begin{pmatrix} 1 \\ X_i - x \end{pmatrix} \alpha_i(x) (Y_i - y)^2.$$

Replacing the Euclidean distance with a metric  $d$ , the random forest weighted local linear Fréchet regression for a general metric space  $(\Omega, d)$  is proposed as

$$\hat{l}_\oplus(x) = \operatorname{argmin}_{y \in \Omega} e_1^T (\tilde{X}^T A \tilde{X})^{-1} \sum_{i=1}^n \begin{pmatrix} 1 \\ X_i - x \end{pmatrix} \alpha_i(x) d^2(Y_i, y). \quad (10)$$

Our proposed local constant and local linear methods are both to calculate weighted Fréchet means, but the weights of local linear method may be negative. In order to study the consistency of  $\hat{l}_\oplus(x)$ , we assume the following conditions.

(A15)  $X \sim \mathcal{U}([0, 1]^p)$ , the uniform distribution on  $[0, 1]^p$ .

(A16)  $N(L_b(x; \mathcal{D}_n^b, \xi_b)) \rightarrow \infty$  for  $b = 1, \dots, B$ .

(A17) The Fréchet trees are trained in such a way that for each  $y \in \Omega$

$$\max_{1 \leq i \leq n, 1 \leq b \leq B} [1 \{X_i \in L_b(x; \mathcal{D}_n^b, \xi_b)\} |M_\oplus(X_i, y) - M_\oplus(x, y)|] \xrightarrow{P} 0.$$

That is, the leaf node containing  $x$  shrink such that the maximal variation of the function  $M_\oplus(\cdot, y)$  within a cell shrinks to 0 in probability for each  $y \in \Omega$ .

(A18)  $m_\oplus(x)$  and  $\hat{l}_\oplus(x)$  exist and are unique, the latter almost surely. For any  $\varepsilon > 0$ ,

$$\inf_{d(y, m_\oplus(x)) > \varepsilon} \{M_\oplus(x, y) - M_\oplus(x, m_\oplus(x))\} > 0.$$

Assumptions (A15)–(A17) are similar to the conditions used in [Bloniarz et al. \(2016\)](#) to establish the consistency of a nonparametric regression estimator using random forests as adaptive nearest neighbor generators. The assumption (A17) is a general condition, which can be deduced from assumptions (A2) and (A3). It is important to note that assumption (A16) is not required for the consistency of our local constant method. But it provides a guarantee that the law of large numbers can be used for the samples in the leaf node, which derives the consistency of  $\hat{l}_\oplus(x)$  even when  $B$  in the random forest kernel is a fixed constant. Another reasonable interpretation is that the random forest provides weights for the final local linear regression and should not be used to model strong, smooth signals to prevent overfitting phenomenon. In other words, the Fréchet trees that form the forest here should not grow too deep. These can also be observed in the simulation part of the appendix, where moderately grown trees can improve the performance of  $\hat{l}_\oplus(x)$ . But our local constant method often requires deeper trees. In addition to the assumptions above, the honesty condition is still necessary to prove consistency of  $\hat{l}_\oplus(x)$ .

**Theorem 5.** Suppose that for a fixed  $x \in [0, 1]^p$ , (A1), (A15)–(A18) hold and Fréchet trees are honest. Then  $\hat{l}_\oplus(x)$  is pointwise consistent, that is,

$$d(\hat{l}_\oplus(x), m_\oplus(x)) = o_p(1).$$

**Remark 3.** As can be seen from Remark 1, we have weakened the requirement of our local constant method for the number  $B$  of trees, which eliminates the gap between theoretical investigations and practical applications. Certainly, if we re-impose the assumptions of local linear method here on it, a parallel proof guarantees that  $B$  can be further weakened to a fixed constant.

After introducing our two methods, we briefly summarize all relevant methods. The classical Nadaraya-Watson regression, random forest, Nadaraya-Watson Fréchet regression ([Hein, 2009](#)) and random forest weighted local constant Fréchet regression (RFWLCFR) are essentially all local constant estimators. The classical local linear regression, random forest weighted local linear regression ([Bloniarz et al., 2016; Friedberg et al., 2020](#)), local Fréchet regression ([Petersen and Müller, 2019](#)) and random forest weighted local linear Fréchet regression (RFWLLFR) are essentially all local linear estimators. The relationship among the eight types of estimators is shown in Fig. 2.

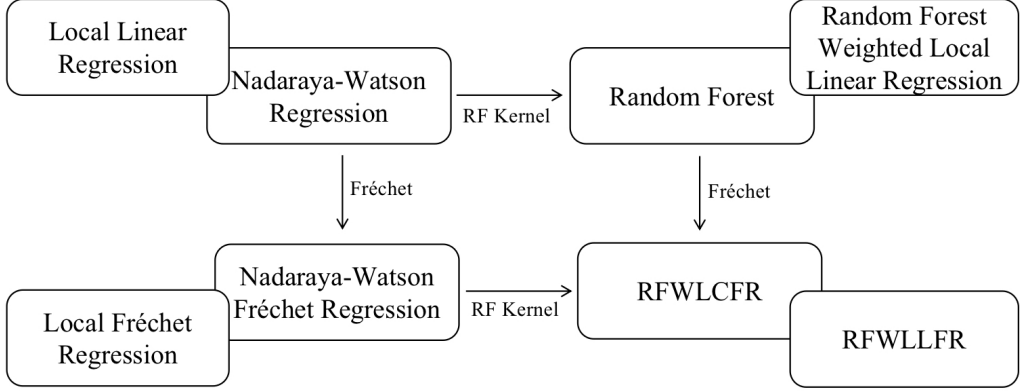


Figure 2: The relationship among the eight local linear estimators.

## 5 Simulations

### 5.1 Some instructions

In this section, we consider three Fréchet regression scenarios including probability distributions, symmetric positive definite matrices, and spherical data to evaluate the performance of the two methods proposed above. We include the global Fréchet regression (GFR) and local Fréchet regression (LFR) (Petersen and Müller, 2019), and the Fréchet random forest (FRF) (Capitaine et al., 2019) for comparisons. Throughout this section, GFR and LFR can be implemented by R-package ‘‘frechet’’ (Chen et al., 2020). And FRF can be implemented by the R-package ‘‘FrechForest’’ (Capitaine, 2021) with a slight modification through adding the three new types of responses and their corresponding metrics into the package. Our random forest weighted local constant Fréchet regression (RFWLCFR) and random forest weighted local linear Fréchet regression (RFWLLFR) are also implemented in R. For simplicity, the Fréchet trees in our simulations are not necessarily honest. All random forests are constructed by 100 Fréchet trees using the criterion introduced in section A.1 of appendix. There are three hyper-parameters for each Fréchet tree: the size  $s_n$  of each subsample, the depth of Fréchet trees and the number of features randomly selected at each internal node. The choice of  $s_n$  is very tedious and time-consuming. Here we instead acquire all subsamples by sampling from the training data set  $\mathcal{D}_n$  with replacement, which commonly used in random forest codes. When the size  $n$  of  $\mathcal{D}_n$  is large enough, each subsample is expected to have the fraction  $(1 - 1/e) \approx 63.2\%$  of the unique examples of  $\mathcal{D}_n$ . We consider  $3 \sim \lceil \log_2 n \rceil$  for the range of tuning about the depth of Fréchet trees, where  $n$  is the number of training samples. For a fair comparison, each method chooses the hyper-parameters by cross-validation.

In the following simulations, each setting is repeated 100 times. For the  $r$ th Monte Carlo test,  $\hat{m}_\oplus^r$  denotes the fitted function based on the method  $\hat{m}_\oplus$  and the quality of the estimation is measured quantitatively by the mean squared error

$$\text{MSE}_r(\hat{m}_\oplus) = \frac{1}{100} \sum_{i=1}^N d^2(\hat{m}_\oplus^r(X_i), m_\oplus(X_i))$$

based on 100 new testing points.

### 5.2 Fréchet Regression for Distributions

Let  $(\Omega, d)$  be the metric space of probability distributions on  $\mathcal{R}$  with finite second order moments and the quadratic Wasserstein metric  $d_W$ . For two such distributions  $Y_1$  and  $Y_2$ , the squared Wasserstein distance is defined by

$$d_W^2(Y_1, Y_2) = \int_0^1 \{Y_1^{-1}(t) - Y_2^{-1}(t)\}^2 dt, \quad (11)$$

where  $Y_1^{-1}$  and  $Y_2^{-1}$  are quantile functions corresponding to  $Y_1$  and  $Y_2$ , respectively.

Let  $X_1, \dots, X_n \sim \mathcal{U}([0, 1]^p)$ , and we generate random normal distribution  $Y$  by

$$Y = \mathcal{N}(\mu_Y, \sigma_Y^2),$$

where  $\mu_Y$  and  $\sigma_Y$  are random variables dependent on  $X$  as described in the following.

Setting I-1:

$$\mu_Y \sim \mathcal{N}(5\beta^T X - 2.5, \sigma^2) \quad \text{and} \quad \sigma_Y = 1.$$

We consider four situations of the dimension of  $X$ :  $p = 2, 5, 10, 20$ .

- (i) For  $p = 2$ :  $\beta = (0.75, 0.25)$ .
- (ii) For  $p = 5, 10$ :  $\beta = (0.1, 0.2, 0.3, 0.4, 0, \dots, 0)$ .
- (iii) For  $p = 20$ :  $\beta = (0.1, 0.2, 0.3, 0.4, 0, \dots, 0, 0.1, 0.2, 0.3, 0.4) / 2$ .

Setting I-2:

$$\mu_Y \sim \mathcal{N}(\sin(4\pi\beta_1^T X)(2\beta_2^T X - 1), \sigma^2) \quad \text{and} \quad \sigma_Y = 2|e_1^T X - e_2^T X|,$$

where  $e_i$  is a vector of zeroes with 1 in the  $i$ th element. We also consider four situations.

- (i) For  $p = 2$ :  $\beta_1 = (0.75, 0.25)$ ,  $\beta_2 = (0.25, 0.75)$ .
- (ii) For  $p = 5, 10, 20$ :  $\beta_1 = (0.1, 0.2, 0.3, 0.4, 0, \dots, 0)$ ,  $\beta_2 = (0, \dots, 0, 0.1, 0.2, 0.3, 0.4)$ .

We set  $n = 100, 200$  for  $p = 2$ ;  $n = 200, 500$  for  $p = 5$ ;  $n = 500, 1000$  for  $p = 10$  and  $n = 1000, 2000$  for  $p = 20$ . For computation simplicity, the quantile function of each  $Y_i$  is discretized as the 21 quantile points corresponding to the equispaced grids on  $[0, 1]$ . It can then be verified from (11) that the Wasserstein distance between the two distributions is actually the Euclidean distance between their quantile points. Therefore, our RFWLCFR and the method FRF will have the same output.

For the fairness of comparison, we begin with the setting I-1 where data are generated by a linear way. It is compliant with the initial assumptions of GFR. The results are recorded in Table 1. Not surprisingly, GFR is the best performer, followed by RFWLLFR. It is worth noting that in all cases, RFWLLFR performs best when the depth of Fréchet trees is 3 (under the constraint  $3 \sim \lceil \log_2 n \rceil$ ) and only one feature is randomly selected at each internal node. In fact, if the input space is not partitioned, *i.e.*, the Fréchet trees are of depth 1, RFWLLFR will do the same thing as GFR except RFWLLFR has a subsampling process from the training data. For setting I-2, as the Fréchet regression function is nonlinear, the performance of GFR is the worst. And we observe that the performance of GFR can not be improved significantly by simply increasing the number of training samples. For the low-dimensional case, the best performance is concentrated in RFWLLFR, indicating that it is easier to capture nonlinear signals. But as the dimension of  $X$  increases, the requirement of data size increases rapidly for local methods and the fitting becomes more challenging. Instead, more straightforward method RFWLCFR begins to outperform RFWLLFR. LFR is a local method relying heavily on kernel smoothing. The “frechet” package can only handle the case where the dimension of  $X$  is less than 2. When  $p = 2$ , the method LFR does not perform as well as RFWLCFR and RFWLLFR. For the effect of noise size  $\sigma$  and the case that the components of  $X$  are correlated, please refer to appendix.

Table 1: Average MSE (standard deviation) of different methods for setting I-1,2 with  $\sigma = 0.2$  for 100 simulation runs

Model	$(p, n)$	GFR	LFR	RFWLCFR/FRF	RFWLLFR
I-1	(2, 100)	0.0014 (0.0012)	0.0688 (0.0707)	0.0269 (0.0071)	0.0031 (0.0015)
	(2, 200)	0.0006 (0.0006)	0.0452 (0.0363)	0.0179 (0.0037)	0.0014 (0.0008)
	(5, 200)	0.0011 (0.0006)	NA	0.0468 (0.0085)	0.0028 (0.0010)
	(5, 500)	0.0005 (0.0003)	NA	0.0299 (0.0049)	0.0011 (0.0004)
	(10, 500)	0.0009 (0.0004)	NA	0.0401 (0.0059)	0.0019 (0.0005)
	(10, 1000)	0.0004 (0.0002)	NA	0.0284 (0.0039)	0.0009 (0.0002)
	(20, 1000)	0.0009 (0.0003)	NA	0.0542 (0.0088)	0.0015 (0.0004)
	(20, 2000)	0.0004 (0.0001)	NA	0.0444 (0.0059)	0.0007 (0.0002)
I-2	(2, 100)	0.3045 (0.0306)	0.0944 (0.0883)	0.0410 (0.0090)	0.0317 (0.0141)
	(2, 200)	0.3023 (0.0278)	0.0745 (0.1550)	0.0254 (0.0050)	0.0186 (0.0073)
	(5, 200)	0.2482 (0.0206)	NA	0.0772 (0.0136)	0.0719 (0.0121)
	(5, 500)	0.2335 (0.0241)	NA	0.0557 (0.0087)	0.0502 (0.0083)
	(10, 500)	0.2416 (0.0261)	NA	0.1053 (0.0195)	0.1134 (0.0171)
	(10, 1000)	0.2438 (0.0297)	NA	0.0901 (0.0174)	0.0927 (0.0148)
	(20, 1000)	0.2442 (0.0245)	NA	0.1399 (0.0260)	0.1554 (0.0197)
	(20, 2000)	0.2456 (0.0286)	NA	0.1257 (0.0238)	0.1337 (0.0194)

### 5.3 Fréchet Regression for Symmetric Positive-definite Matrices

Let  $(\Omega, d)$  be the metric space  $\mathcal{S}_m^+$  of  $m \times m$  symmetric positive-definite matrices endowed with metric  $d$ . There are many options for metrics, this section focuses on the Log-Cholesky metric and the affine-invariant metric, which both have many good properties (Lin, 2019).

We generate  $X_1, \dots, X_n$  from the uniform distribution  $\mathcal{U}([0, 1]^p)$ . And the response  $Y$  is generated via symmetric matrix variate normal distribution (Zhang et al., 2021). Consider the simplest case, we say an  $m \times m$  symmetric matrix

$A \sim \mathcal{N}_{mm}(M; \sigma^2)$  if  $A = \sigma^2 Z + M$  where  $M$  is an  $m \times m$  symmetric matrix and  $Z$  is an  $m \times m$  symmetric random matrix with independent  $\mathcal{N}(0, 1)$  diagonal elements and  $\mathcal{N}(0, 1/2)$  off-diagonal elements. We consider the following settings with  $Y$  being symmetric positive-definite matrices.

Setting II-1:

$$\log(Y) \sim \mathcal{N}_{mm}(\log(D(X)), \sigma^2)$$

with  $D(X) = \exp \begin{pmatrix} 1 & \rho(X) \\ \rho(X) & 1 \end{pmatrix}$ ,  $\rho(X) = \cos(4\pi(\beta^T X))$ . The choice of  $\beta$  corresponds to  $p = 2, 5, 10, 20$  is the same as setting I-1.

Setting II-2:

$$\log(Y) \sim \mathcal{N}_{mm}(\log(D(X)), \sigma^2)$$

with  $D(X) = \begin{pmatrix} 1 & \rho_1(X) & \rho_2(X) \\ \rho_1(X) & 1 & \rho_1(X) \\ \rho_2(X) & \rho_1(X) & 1 \end{pmatrix}$ ,  $\rho_1(X) = 0.8 \cos(4\pi(\beta_1^T X))$ ,  $\rho_2(X) = 0.4 \cos(4\pi(\beta_2^T X))$ . The choice of  $(\beta_1, \beta_2)$  corresponds to  $p = 2, 5, 10, 20$  is the same as setting I-2.

We again compare our methods with GFR, LFR and FRF. Since the Log-Cholesky distance between two symmetric positive-definite matrices is essentially the Frobenius distance between the matrices after some transformations. Therefore, similar to the regression for distributions, RFWLCFR and FRF would have the same output. Results about setting II-1,2 with Log-Cholesky metric are showed in Table 2. When  $p = 2$ , LFR has the best performance. When  $p > 2$ , RFWLLFR performs the best in most cases. The results with the affine-invariant metric summarized in Table 3 also advocates RFWLLFR. Moreover, for the affine-invariant metric, we observe slight differences between RFWLCFR and FRF.

Table 2: Average MSE (standard deviation) of different methods for setting II-1,2 with  $\sigma^2 = 0.2$  and Log-Cholesky metric for 100 simulation runs

Model	$(p, n)$	GFR	LFR	RFWLCFR/FRF	RFWLLFR
II-1	(2, 100)	1.264 (0.116)	0.088 (0.039)	0.177 (0.061)	0.128 (0.072)
	(2, 200)	1.209 (0.089)	0.038 (0.016)	0.082 (0.019)	0.054 (0.019)
	(5, 200)	1.281 (0.115)	NA	0.507 (0.082)	0.397 (0.096)
	(5, 500)	1.267 (0.104)	NA	0.299 (0.046)	0.190 (0.040)
	(10, 500)	1.279 (0.104)	NA	0.586 (0.101)	0.575 (0.101)
	(10, 1000)	1.253 (0.096)	NA	0.420 (0.084)	0.407 (0.082)
	(20, 1000)	0.973 (0.114)	NA	0.623 (0.088)	0.485 (0.075)
	(20, 2000)	0.956 (0.122)	NA	0.522 (0.076)	0.379 (0.058)
II-2	(2, 100)	1.932 (0.135)	0.240 (0.098)	0.367 (0.068)	0.283 (0.079)
	(2, 200)	1.898 (0.152)	0.109 (0.020)	0.188 (0.035)	0.143 (0.032)
	(5, 200)	1.980 (0.136)	NA	0.855 (0.114)	0.674 (0.116)
	(5, 500)	1.935 (0.143)	NA	0.543 (0.065)	0.369 (0.048)
	(10, 500)	1.971 (0.136)	NA	1.057 (0.155)	1.056 (0.134)
	(10, 1000)	1.949 (0.140)	NA	0.845 (0.134)	0.839 (0.119)
	(20, 1000)	1.970 (0.116)	NA	1.251 (0.200)	1.362 (0.171)
	(20, 2000)	1.962 (0.140)	NA	1.071 (0.178)	1.191 (0.158)

## 5.4 Fréchet regression for spherical data

Let  $(\Omega, d)$  be the metric space  $\mathbb{S}^2$  of sphere data endowed with the geodesic distance  $d_g$ . For two points  $Y_1, Y_2 \in \mathbb{S}^2$ , the geodesic distance is defined by

$$d_g(Y_1, Y_2) = \arccos(Y_1^T Y_2).$$

We generate i.i.d  $X_1, \dots, X_n \sim \mathcal{U}([0, 1]^p)$ . And  $Y_i$  are generated by the following two settings.

Setting III-1: Let the Fréchet regression function be

$$m_{\oplus}(X) = (\{1 - (\beta_1^T X)^2\}^{1/2} \cos(\pi(\beta_2^T X)), \{1 - (\beta_1^T X)^2\}^{1/2} \sin(\pi(\beta_2^T X)), \beta_1^T X)^T.$$

We generate binary Normal noise  $\varepsilon_i$  on the tangent space  $T_{m_{\oplus}(X_i)}\mathbb{S}^2$ , then map  $\varepsilon_i$  back to  $\mathbb{S}^2$  by Riemannian exponential map to get  $Y_i$ . Specifically, we first independently generate  $\delta_{i1}, \delta_{i2} \stackrel{iid}{\sim} \mathcal{N}(0, 0.2^2)$ , then let  $\varepsilon_i = \delta_{i1}v_1 + \delta_{i2}v_2$ , where

Table 3: Average MSE (standard deviation) of different methods for setting II-1,2 with  $\sigma^2 = 0.2$  and affine-invariant metric for 100 simulation runs

Model	$(p, n)$	FRF	RFWLCFR	RFWLLFR
II-1	(2, 100)	0.164133 (0.041988)	0.164132 (0.041991)	0.124380 (0.046016)
	(2, 200)	0.080703 (0.015133)	0.080707 (0.015134)	0.063739 (0.016001)
	(5, 200)	0.408030 (0.063235)	0.408010 (0.063239)	0.332478 (0.073828)
	(5, 500)	0.243664 (0.035725)	0.243662 (0.035725)	0.166254 (0.029714)
	(10, 500)	0.501018 (0.079189)	0.500904 (0.079182)	0.464811 (0.079191)
	(10, 1000)	0.366349 (0.069003)	0.366257 (0.068997)	0.331014 (0.067757)
	(20, 1000)	0.502299 (0.073056)	0.502238 (0.073048)	0.390836 (0.057455)
	(20, 2000)	0.425098 (0.062546)	0.425046 (0.062547)	0.304537 (0.044358)
II-2	(2, 100)	0.286285 (0.059663)	0.286285 (0.059655)	0.238548 (0.062099)
	(2, 200)	0.154080 (0.025816)	0.154085 (0.025813)	0.128763 (0.023595)
	(5, 200)	0.627837 (0.088528)	0.627769 (0.088545)	0.499721 (0.087616)
	(5, 500)	0.396012 (0.046278)	0.395999 (0.046281)	0.280171 (0.035996)
	(10, 500)	0.794744 (0.128331)	0.794220 (0.128334)	0.762684 (0.100195)
	(10, 1000)	0.638420 (0.110770)	0.637765 (0.110686)	0.605356 (0.089589)
	(20, 1000)	0.927755 (0.147346)	0.927363 (0.147369)	0.991135 (0.111894)
	(20, 2000)	0.795528 (0.141159)	0.795009 (0.141150)	0.878269 (0.118397)

$\{v_1, v_2\}$  forms an orthogonal basis of tangent space  $T_{m_{\oplus}(X_i)} \mathbb{S}^2$ . Then  $Y_i$  can be generated by

$$Y_i = \text{Exp}_{m_{\oplus}(X_i)}(\varepsilon_i) = \cos(\|\varepsilon_i\|) m_{\oplus}(X_i) + \sin(\|\varepsilon_i\|) \frac{\varepsilon_i}{\|\varepsilon_i\|} \quad (i = 1, \dots, n),$$

where  $\|\cdot\|$  is the Euclidean norm. Consider the following four kinds of dimensions

- (i) For  $p = 2$ :  $\beta_1 = (1, 0), \beta_2 = (0, 1)$ .
- (ii) For  $p = 5, 10, 20$ :  $\beta_1 = (0.1, 0.2, 0.3, 0.4, 0, \dots, 0), \beta_2 = (0, \dots, 0, 0.1, 0.2, 0.3, 0.4)$ .

Setting III-2: Consider the following model

$$Y_i = (\sin(\beta_1^T X_i + \varepsilon_{i1}) \sin(\beta_2^T X_i + \varepsilon_{i2}), \sin(\beta_1^T X_i + \varepsilon_{i1}) \cos(\beta_2^T X_i + \varepsilon_{i2}), \cos(\beta_1^T X_i + \varepsilon_{i1}))^T,$$

where the random noise  $\varepsilon_{i1}, \varepsilon_{i2} \stackrel{iid}{\sim} \mathcal{N}(0, 0.2^2)$  are generated independently. The four situations correspond to  $p = 2, 5, 10, 20$  are the same as setting III-1.

Setting III-1 is similar to [Petersen and Müller \(2019\)](#) and [Zhang et al. \(2021\)](#), and setting III-2 is similar to [Ying and Yu \(2022\)](#). For Fréchet regression with sphere data, we focus on the comparison of FRF, RFWLCFR and RFWLLFR. RFWLCFR and FRF will have different outputs under the geodesic distance  $d_g$ . We summarize the estimation error in the appendix due to space limitations. To vividly describe the performance of RFWLCFR and RFWLLFR, Fig. 3 exhibits the prediction of nine given testing points with  $p = 2$  and  $n = 200$  for setting III-1,2, which verifies the advantage of RFWLLFR.

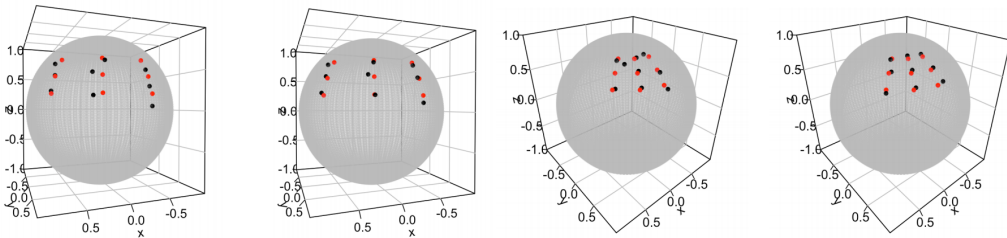


Figure 3: The plots of predictions of  $m_{\oplus}(x)$  given by RFWLCFR (the 1st and 3rd panels) and RFWLLFR (the 2nd and 4th panels) in a simulation run of  $p = 2, n = 200$ . The left two panels show results of setting III-1, while the right two show results of setting III-2. The red points represent real points, and the black points represent predicted points.

## 6 Real Application

Taking distribution as the outcome of interest allows us to obtain more information than summary statistics. In this section, we apply the two methods proposed in this paper to deal with the Fréchet regression problem for human

mortality distribution. Just like [Zhang et al. \(2021\)](#), we also consider the following 9 predictor variables: (1) Population Density: population per square Kilometer; (2) Sex Ratio: number of males per 100 females in the population; (3) Mean Childbearing Age: the average age of mothers at the birth of their children; (4)Gross Domestic Product (GDP) per Capita; (5) Gross Value Added (GVA) by Agriculture: the percentage of agriculture, hunting, forestry, and fishing activities of gross value added; (6) Consumer price index: treat 2010 as the base year; (7) Unemployment Rate; (8) Expenditure on Health (percentage of GDP); (9) Arable Land (percentage of total land area). These variables involve population, economy, health, and geography factors in 2015, which are closely related to human mortality. The data are collected from United Nation Databases (<http://data.un.org/>) and UN World Population Prospects 2019 Databases (<https://population.un.org/wpp/Download>). The life table considered here contains the number of deaths for each single age group from 162 countries in 2015. We treat the life table data as histograms of death versus age, with bin width equal to one year (the results of subsequent analysis are similar when bin width is set to five years). Then the package “frechet” helps to transform the histograms to smoothed probability density functions. For comparison, we also implement GFR, LFR and FRF. Since the R-package of LRF is only applicable to the case where  $X$  does not exceed 2-dimensions, an effective solution is to consider the Fréchet sufficient dimension reduction method weighted inverse regression ensemble (WIRE) proposed by [Ying and Yu \(2022\)](#). The first four largest singular values of the WIRE matrix ([Ying and Yu, 2022](#)) are 4.486, 0.785, 0.101, 0.066 and we determine the dimension of central space to be 2. And the first two sufficient dimension reduction directions obtained by WIRE are

$$\hat{\beta}_1 = (-0.092, -0.084, 0.009, -0.429, 0.806, 0.048, 0.104, -0.364, -0.076)^T;$$

$$\hat{\beta}_2 = (0.103, 0.079, 0.641, 0.566, 0.415, -0.017, 0.130, 0.243, 0.066)^T.$$

The two directions transform the 9-dimensional  $X$  into a 2-dimensional vector  $(\hat{\beta}_1^T X, \hat{\beta}_2^T X)$  as the input of LRF.

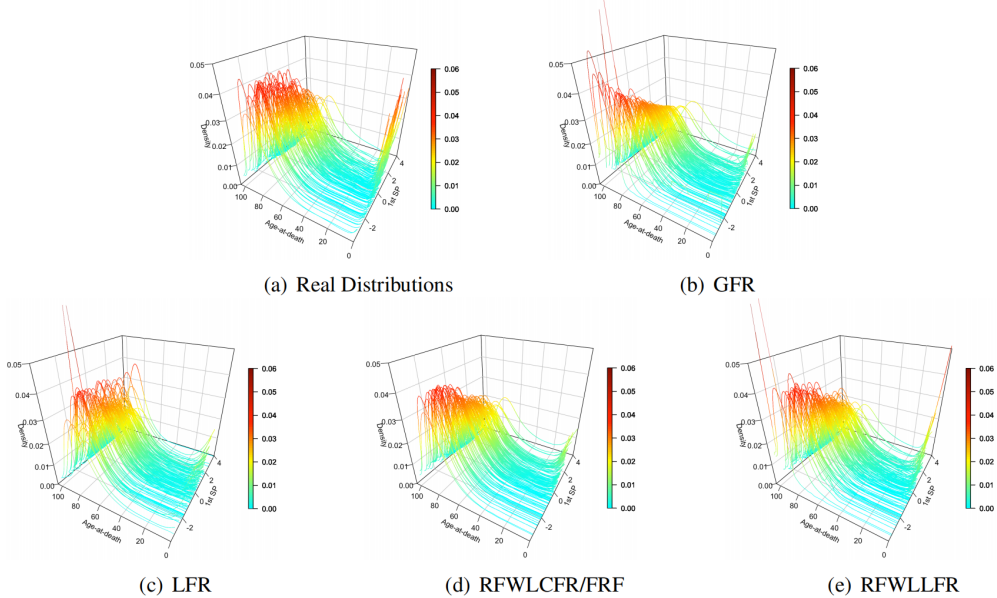


Figure 4: The plot (a) is the real mortality distributions against the first sufficient predictor, and the remaining plots are the distributions predicted by each method against the sufficient predictor.

We then perform 9-fold testing to evaluate the performance of all Fréchet regression methods. Specifically, we divide the 162 countries into 9 parts evenly and conduct 9 training runs. For each run, one of 9 parts is chosen as the testing set and the rest as the training set. The test errors (mean squared errors based on the Wasserstein distance) obtained for nine runs are averaged for each method. The average test errors are recorded as 56.51 for GFR, 41.66 for LFR, 31.79 for RFWLCFR/FRF, and 36.20 for RFWLLFR. RFWLCFR/FRF has the best performance. This reflects that inadequate sample size and large variation across countries increase the difficulty of the 9-dimensional local Fréchet regression problem.

To show the performance of each method more vividly, we aid the analysis by plotting the mortality density predictions against the first sufficient predictor  $\hat{\beta}_1^T X$  (see Fig. 4). For reference, the plot (a) of Fig. 4 is the smooth real density functions fitted according to the human mortality data. Observations reveal that the first sufficient predictor represents the development degree of a country. Countries with large  $\hat{\beta}_1^T X$  have backward medical level and indigent living conditions, resulting in higher infant mortality and lower life expectancy. It is clear from plots that the distribution in the elderly age region (80 ~ 100 years old) and the infant age region (near 0 years old) is challenging to be well estimated. GFR performs poorly in both regions. It underestimates the infant mortality rate, but succeeds in exhibiting a tendency to concentrate the distribution toward the elderly age region as the first sufficient predictor decreases. Compared with GFR, LFR based

solely on two sufficient dimension reduction directions improves predictions of the elderly age region, but deteriorates for the infant age region due to the boundary effect of the local method. In terms of the overall visual effect, the predictions of RFWLCFR/FRF are closest to the real distributions, but still suffer from severe boundary effect. Among all local methods, RFWLLFR has the best performance in the infant age region, showing that the local linear method mitigates the boundary effect to some extent. RFWLLFR performs slightly inferior to RFWLCFR in the elderly age region, but much better than LFR. Overall speaking, RFWLCFR has a remarkable advantage in this real data application. It again reflects the fact that RFWLLRF is not always the best choice, especially for complex regression problems with a small amount of data. RFWLCFR tends to be more robust and accurate in these cases.

## 7 Discussion

We provide two flexible and complementary Fréchet regression estimators based on random forests, which mitigate the curse of dimensionality for local Fréchet regression. And the two methods certainly extend random forests to the case with metric space valued responses. We also establish the consistency, asymptotic convergence rate, and asymptotic normality of the proposed random forest weighted local constant Fréchet regression estimator. Moreover, our theoretical findings include the most updated theoretical result of Euclidean random forests as a special case. The theory developed for  $M_{m_n}$ -estimator based on infinite order U-processes and U-Statistics is of independent interest. Numerical performance demonstrated in both simulation studies and real applications advocates our proposals.

In the present work, we focus on the theory of random forest weighted local constant Fréchet regression estimator. Theoretical investigation into the random forest weighted local linear Fréchet regression estimator including convergence rate and asymptotic normality is challenging. We leave it to future research. Considering suitable ridge penalties as suggested by [Friedberg et al. \(2020\)](#) in combination with our local linear method should be helpful for further achieving asymptotic normality. Moreover, uniform convergence rates of our proposals deserve further delicate analysis.

For Fréchet regression, our two methods only use the most basic information of a metric space. So our methods have a wide range of applicability. When the metric space is a specific Riemannian manifold, more information can be considered in the construction of the model. Taylor expansions can be implemented on the tangent plane of the Riemannian manifold based on some specific geometric structure. And some advanced statistical tools designed for responses lying on the Riemannian manifold were developed, like the intrinsic local polynomial regression ([Yuan et al., 2012](#)) and the manifold additive model ([Lin et al., 2022](#)). For metric space being a specific Hilbert space, vector operations and an inner product structure are available, which inspires several promising nonparametric Hilbertian regression such as [Jeon and Park \(2020\)](#) and [Jeon et al. \(2022\)](#). For the above two types of responses, we can consider a nonparametric regression framework based on the random forest kernel in the future. When more information of the output space is considered, models are expected to be more specific and targeted.

## A More Explanation of Some Concepts

### A.1 Fréchet tree with adaptive splitting criterion

A regression tree  $T$  splits the input space recursively from the root node (the entire input space). At each split, the parent node is divided into two child nodes along a certain feature direction and a certain cutoff point, which are decided by a specific splitting criterion. After many splits, the child node becomes small enough to form a leaf node, and the sample data points within the leaf node are used to estimate the conditional (Fréchet) mean.

We refer to all regression trees with metric space valued responses as Fréchet trees regardless of their splitting criterion. Here we consider the adaptive criterion–variance reduction splitting criterion, which utilizes both the information of predictor  $X = (X^{(1)}, \dots, X^{(p)})$  and response  $Y$  in the node splitting decision. The impurity of  $Y$  from a general metric space is no longer measured by the variance under the Euclidean distance. Instead, we use the Fréchet variance. A split on an internal node  $A$  can be represented by a pair  $(j, c)$ ,  $j \in \{1, \dots, p\}$ , indicating that  $A$  is split at position  $c$  along the direction of feature  $j$ . We select the optimal  $(j_n^*, c_n^*)$  to decrease the sample Fréchet variance as much as possible, so that the sample points in the same child node have great similarity. The splitting criterion is

$$\mathcal{L}_n(j, c) = \frac{1}{N_n(A)} \left\{ \sum_{i: X_i \in A} d^2(Y_i, \bar{Y}_A) - \sum_{i: X_i \in A_{j,l}} d^2(Y_i, \bar{Y}_{A_{j,l}}) - \sum_{i: X_i \in A_{j,r}} d^2(Y_i, \bar{Y}_{A_{j,r}}) \right\}$$

where  $A_{j,l} = \{x \in A : x^{(j)} < c\}$ ,  $A_{j,r} = \{x \in A : x^{(j)} \geq c\}$ ,  $N_n(A)$  is the number of observations falling into the node  $A$ , and  $\bar{Y}_A = \operatorname{argmin}_{y \in \Omega} \sum_{i: X_i \in A} d^2(Y_i, y)$ , i.e., the sample Fréchet mean of  $Y_i$ 's associated to the observations belonging to the node  $A$ .  $\bar{Y}_{A_{j,l}}$  and  $\bar{Y}_{A_{j,r}}$  are defined similarly. Then the optimal split pair is decided by

$$(j_n^*, c_n^*) = \operatorname{argmax}_{j,c} \mathcal{L}_n(j, c).$$

The above process to find the optimal split is accurate but computationally intensive. In all simulation experiment of this paper, we adopt another efficient way introduced by [Capitaine et al. \(2019\)](#). A split on an internal node  $A$  along the direction of feature  $j$  is any couple of distinct elements  $(c_{j,l}, c_{j,r})$ . The partition associated with elements  $(c_{j,l}, c_{j,r})$  is defined by  $A_{j,l} = \{x \in A : |x^{(j)} - c_{j,l}| \leq |x^{(j)} - c_{j,r}|\}$  and  $A_{j,r} = \{x \in A : |x^{(j)} - c_{j,r}| < |x^{(j)} - c_{j,l}|\}$ , the left and right child nodes of the node  $A$ . Again, let

$$\mathcal{H}_n(j) = \frac{1}{N_n(A)} \left\{ \sum_{i:X_i \in A} d^2(Y_i, \bar{Y}_A) - \sum_{i:X_i \in A_{j,l}} d^2(Y_i, \bar{Y}_{A_{j,l}}) - \sum_{i:X_i \in A_{j,r}} d^2(Y_i, \bar{Y}_{A_{j,r}}) \right\}.$$

Then the optimal split  $(c_{j_n^*,l}, c_{j_n^*,r})$  is decided by

$$j_n^* = \operatorname{argmax}_j \mathcal{H}_n(j).$$

To determinate the representatives  $(c_{j,l}, c_{j,r})$ , the 2-means algorithm ( $k$ -means with  $k = 2$ ) can be implemented on the  $j$ th component of the sample points falling into the node  $A$ .

When the construction of the tree  $T$  is completed, let  $L_T(x)$  be the leaf node of  $T$  containing  $X = x$ . Then  $m_{\oplus}(x)$  can be possibly estimated by the sample Fréchet mean of  $Y_i$ 's corresponding to the observations belonging to  $L_T(x)$ , that is

$$\hat{m}_{\oplus}(x) = \operatorname{argmin}_{y \in \Omega} \sum_{i:X_i \in L_T(x)} d^2(Y_i, y).$$

## A.2 Random forest kernel

Nadaraya-Watson Fréchet regression ([Hein, 2009](#)) and local Fréchet regression ([Petersen and Müller, 2019](#)) are based on the rationality that  $(X, Y)$  should be informative for  $m_{\oplus}(x)$  if  $X$  is close to  $x$  (assume the function  $m_{\oplus}$  has some degree of smoothness). The smoothing kernel  $K_h(X_i - x)$  is exactly used to weight the contribution of each  $(X_i, Y_i)$  to the estimation of  $m_{\oplus}(x)$  according to the proximity of  $X_i$  to  $x$ . But if the predictor contains some irrelevant variables, using the classical kernel smoothing functions often has unsatisfactory performance.

Different from the above kernel, the random forest kernel has a different mechanism of generating local weights. Fréchet trees produce local relationships among samples by recursively partitioning the input space. In addition to helping combat the curse of dimensionality, the random forest kernel can be adaptive if the partition process makes use of the information from responses  $Y$ , for example, the variance reduction splitting criterion introduced above. For the sample points divided into the same child node (or leaf), it is required that not only the distance of  $X$  is close to each other, but also the sample Fréchet variance of  $Y$  is small. It encourages Fréchet trees to select more relevant variables to divide the sample space. So the contribution value of  $(X_i, Y_i)$  given by the random forest kernel  $\alpha_i(x)$  is jointly determined by both the information of  $X_i$  and  $Y_i$ . The random forest kernel prefers to assign high weight to sample points that share a similar value of the response.

Assuming each tree is trained with at most  $k$  sample points per leaf node, and the full training data is used for each tree, [Lin and Jeon \(2006\)](#) introduced a paradigm to understand Euclidean random forests by considering any sample points falling into the leaf  $L(x)$  be a  $k$  potential nearest neighbor ( $k$ -PNN) of  $x$ . When the splitting scheme of trees depends on the response,  $k$ -PNNs are chosen by an adaptive selection scheme. And a  $k$ -potential nearest neighbor can be made a  $k$  nearest neighbor by choosing a reasonable distance metric but not simple Euclidean distance. The adoptive nature of the random forest kernel can be reflected in this way. And the similar analysis can be extended to non-Euclidean cases.

## A.3 The difference between random forest weighted local constant Fréchet regression and Fréchet random forest ([Capitaine et al., 2019](#))

We illustrate the difference between these two methods from the generalization of Euclidean random forests. For the Euclidean random forest constructed by a total number of  $B$  randomized regression trees,

$$\text{RF}(x) = \frac{1}{B} \sum_{b=1}^B T_b(x; \mathcal{D}_n^b, \xi_b) = \frac{1}{B} \sum_{b=1}^B \left\{ \frac{1}{N(L_b(x; \mathcal{D}_n^b, \xi_b))} \sum_{i:X_i \in L_b(x; \mathcal{D}_n^b, \xi_b)} Y_i \right\}. \quad (12)$$

From the kernel perspective, the Euclidean random forest can be expressed by

$$\text{RF}(x) = \sum_{i=1}^n \alpha_i(x) Y_i, \quad (13)$$

where  $\alpha_i(x) = \frac{1}{B} \sum_{b=1}^B \frac{1_{\{X_i \in L_b(x; \mathcal{D}_n^b, \xi_b)\}}}{N(L_b(x; \mathcal{D}_n^b, \xi_b))}$  is the random forest kernel.

There are two generalization methods corresponding to the two views (12) and (13) of the random forest above. We first rewrite the explicit expression of the random forest estimator (12) as the implicit minimizer of certain objective functions.

$$\text{RF}(x) = \operatorname{argmin}_{y \in \mathcal{R}} \frac{1}{B} \sum_{b=1}^B \left[ \operatorname{argmin}_{y \in \mathcal{R}} \left\{ \frac{1}{N(L_b(x; \mathcal{D}_n^b, \xi_b))} \sum_{i: X_i \in L_b(x; \mathcal{D}_n^b, \xi_b)} (Y_i - y)^2 \right\} - y \right]^2.$$

Then the first generalization to metric space valued response is simply replacing the Euclidean distance by the metric  $d$  of  $\Omega$ , that is,

$$\text{RF}_{\oplus}^{(1)}(x) = \operatorname{argmin}_{y \in \Omega} \frac{1}{B} \sum_{b=1}^B d^2 \left( \operatorname{argmin}_{y \in \Omega} \frac{1}{N(L_b(x; \mathcal{D}_n^b, \xi_b))} \sum_{i: X_i \in L_b(x; \mathcal{D}_n^b, \xi_b)} d^2(Y_i, y), y \right). \quad (14)$$

Alternatively, we can start from (13) and rewrite the random forest estimator as

$$\text{RF}(x) = \operatorname{argmin}_{y \in \mathcal{R}} \sum_{i=1}^n \alpha_i(x) (Y_i - y)^2.$$

We propose the second generalization for metric space valued responses as

$$\text{RF}_{\oplus}^{(2)}(x) = \operatorname{argmin}_{y \in \Omega} \sum_{i=1}^n \alpha_i(x) d^2(Y_i, y). \quad (15)$$

The first generalization (14) is actually the Fréchet random forest proposed by [Capitaine et al. \(2019\)](#). The idea behind this is to average the results of each Fréchet tree. However, our proposed second generalization (15) called random forest weighted local constant Fréchet regression looks more concise because it involves only one “argmin”. To acquire the random forest kernel  $\alpha_i(x)$ , we still need to construct all Fréchet trees. It is worth noting that when  $\Omega = \mathcal{R}$ , (14) and (15) are equivalent. However, for general metric space  $(\Omega, d)$ , (14) and (15) may not be the same. Based on the second type of generalization, we can rigorously establish the complete asymptotic theory. And these results fill the theoretical gap left in [Capitaine et al. \(2019\)](#).

#### A.4 Honest tree

The honesty assumption is the largest divergence between the theory and applications of random forests. But it is necessary for pointwise asymptotic theoretical analysis as it can help to eliminate bias. Similar assumptions have been used in many literature ([Friedberg et al., 2020](#); [Bloniarz et al., 2016](#); [Denil et al., 2013](#); [Biau, 2012](#)). The training examples whose  $Y_i$ 's are used for prediction are called prediction points, while the training examples whose  $Y_i$ 's are used to construct the tree are called structure points. A random forest is honest if it is composed of honest trees. The advantage of such random forests is that the model construction process and prediction process are independent. This brings great convenience to the analysis of the theoretical property of random forests. [Wager and Athey \(2018\)](#) achieved both consistency and the central limit theorem of honest random forests provided that the honesty assumption guarantees the following critical relationship for the bias analysis

$$E\{T(x; \mathcal{D}_n^b, \xi_b)\} = E[E\{Y | X \in L(x; \mathcal{D}_n^b, \xi_b)\}],$$

where  $T(x; \mathcal{D}_n^b, \xi_b)$  is the prediction at  $x$  of the tree constructed by a subsample  $\mathcal{D}_n^b$  and a random draw  $\xi_b \sim \Xi$ , and  $L(x; \mathcal{D}_n^b, \xi_b)$  is the corresponding leaf node containing  $x$  of  $T_b$ . Moreover, their theoretical results can apply to a wide range of random forest algorithms, including the classical variance reduction splitting criterion.

Any method of constructing an honest tree can be applied exactly to the Fréchet trees. The simplest way to achieve honesty is that the splitting rule of trees only depends on the predictor  $X$  like purely random forests ([Arlot and Genuer, 2014](#); [Genuer, 2012](#)). When treating the random forest as a local weighting generator, all training examples in  $L(x)$  can be used to calculate the random forest kernel. If the information of  $Y$  is also considered, then the double-sample tree (outlined in Procedure 1 of [Wager and Athey \(2018\)](#)) is a common approach to generate an honest tree. It divides the training sample into two non-overlapping parts: the structure set  $\mathcal{J}_b$  and the prediction set  $\mathcal{I}_b$  satisfying  $|\mathcal{J}_b| = \lceil s_n/2 \rceil$  and  $|\mathcal{I}_b| = \lfloor s_n/2 \rfloor$ . During the tree growing process, the splits are chosen using any data from the sample  $\mathcal{J}_b$  and  $X$ -observations from the sample  $\mathcal{I}_b$ , but without using  $Y$ -observations from the sample  $\mathcal{I}_b$ . And the estimation of leaf-wise responses only adopts  $Y$ -observations from the sample  $\mathcal{I}_b$ . When treating the random forest as a local weighting generator, we only consider the subset  $\{(X_i, Y_i) : (X_i, Y_i) \in L_b(x)\}$  of  $\mathcal{I}_b$  to calculate the random forest kernel; For more discussion, please refer to section 2.4 and Appendix B of [Wager and Athey \(2018\)](#) or section 2.3 of [Friedberg et al. \(2020\)](#). It is worth noting that if honesty is achieved by double-sample trees, another condition  $\alpha$ -regular mentioned in the paper should be satisfied for the sample  $\mathcal{I}_b$ . This is why  $X$ -observations from the sample  $\mathcal{I}_b$  may be used during the construction of trees.

## A.5 A little remark about random forest weighted local linear Fréchet regression

Consider a special case with  $p = 1$ , then the random forest weighted local linear Fréchet regression estimator  $\hat{l}_\oplus(x)$  has the following equivalent expression.

$$\begin{aligned}
\hat{l}_\oplus(x) &= \operatorname{argmin}_{y \in \Omega} \sum_{i=1}^n e_1^T (\tilde{X}^T A \tilde{X})^{-1} \begin{pmatrix} 1 \\ X_i - x \end{pmatrix} \alpha_i(x) d^2(Y_i, y) \\
&= \operatorname{argmin}_{y \in \Omega} \sum_{i=1}^n e_1^T \begin{pmatrix} \sum_{i=1}^n \alpha_i(x) \\ \sum_{i=1}^n \alpha_i(x)(X_i - x) \quad \sum_{i=1}^n \alpha_i(x)(X_i - x)^2 \end{pmatrix}^{-1} \times \\
&\quad \begin{pmatrix} 1 \\ X_i - x \end{pmatrix} \alpha_i(x) d^2(Y_i, y) \\
&= \operatorname{argmin}_{y \in \Omega} \frac{1}{n} \sum_{i=1}^n e_1^T \begin{pmatrix} \hat{\mu}_0 & \hat{\mu}_1 \\ \hat{\mu}_1 & \hat{\mu}_2 \end{pmatrix}^{-1} \begin{pmatrix} 1 \\ X_i - x \end{pmatrix} \alpha_i(x) d^2(Y_i, y) \\
&= \operatorname{argmin}_{y \in \Omega} \frac{1}{n} \sum_{i=1}^n e_1^T \frac{1}{\hat{\mu}_0 \hat{\mu}_2 - \hat{\mu}_1^2} \begin{pmatrix} \hat{\mu}_2 & -\hat{\mu}_1 \\ -\hat{\mu}_1 & \hat{\mu}_0 \end{pmatrix} \begin{pmatrix} 1 \\ X_i - x \end{pmatrix} \alpha_i(x) d^2(Y_i, y) \\
&= \operatorname{argmin}_{y \in \Omega} \frac{1}{n} \sum_{i=1}^n \frac{1}{\hat{\mu}_0 \hat{\mu}_2 - \hat{\mu}_1^2} \{ \hat{\mu}_2 - \hat{\mu}_1 (X_i - x) \} \alpha_i(x) d^2(Y_i, y) \\
&= \operatorname{argmin}_{y \in \Omega} \frac{1}{n} \sum_{i=1}^n t_{in}(x) d^2(Y_i, y)
\end{aligned}$$

where  $t_{in}(x) = \frac{1}{\hat{\mu}_0 \hat{\mu}_2 - \hat{\mu}_1^2} \alpha_i(x) \{ \hat{\mu}_2 - \hat{\mu}_1 (X_i - x) \}$ ,  $\hat{\mu}_j = \frac{1}{n} \sum_{i=1}^n \alpha_i(x) (X_i - x)^j$ . Apart from the weight generating function, this form coincides with the local Fréchet regression proposed by [Petersen and Müller \(2019\)](#). Acquiring the local Fréchet regression estimators by directly from the corresponding explicit Euclidean forms as we do may be more straightforward.

## A.6 Log-Cholesky metric and affine-invariant metric of symmetric positive-definite matrices

For a matrix  $Y$ , let  $[Y]$  denote the strictly lower triangular matrix of  $Y$ ,  $\mathbb{D}(Y)$  denote the diagonal part of  $Y$  and  $\|Y\|_F$  denote the Frobenius norm. It is well known that if  $Y$  is a symmetric positive-definite matrix, there is a lower triangular matrices  $P$  whose diagonal elements are all positive such that  $PP^T = Y$ . This  $P$  is called the Cholesky factor of  $Y$ , devoted as  $\mathcal{L}(Y)$ .

For an  $m \times m$  symmetric matrix  $A$ ,  $\exp(A) = I_m + \sum_{j=1}^{\infty} \frac{1}{j!} A^j$  is a symmetric positive-definite matrix. Conversely, for a symmetric positive-definite matrix  $Y$ , the matrix logarithmic map is  $\log(Y) = A$  such that  $\exp(A) = Y$ .

For two symmetric positive-definite matrices  $Y_1$  and  $Y_2$ , the Log-Cholesky metric ([Lin, 2019](#)) is defined by

$$d_L(Y_1, Y_2) = d_{\mathcal{L}}(\mathcal{L}(Y_1), \mathcal{L}(Y_2)),$$

where  $d_{\mathcal{L}}(P_1, P_2) = \{ \| [P_1] - [P_2] \|_F^2 + \|\log \mathbb{D}(P_1) - \log \mathbb{D}(P_2)\|_F^2 \}^{1/2}$ . And the affine-invariant metric ([Moakher, 2005; Pennec et al., 2006](#)) is defined by

$$d_A(Y_1, Y_2) = \left\| \log \left( Y_1^{-1/2} Y_2 Y_1^{-1/2} \right) \right\|_F.$$

In practical applications, we need to choose the appropriate metric according to the need. The Log-Cholesky metric is faster in calculation, while the affine-invariant metric has the congruence invariance property. More discuss refers to [Lin \(2019\)](#).

## B Additional Simulations

### B.1 Fréchet Regression for Distributions

Random forest weighted local constant Fréchet regression (RFWLCFR) is similar in nature to random forests, so it prefers using deeper Fréchet trees. As for random forest weighted local linear Fréchet regression (RFWLLFR), knowing that a more powerful local linear regression will be used for the final model fitting, it is not reasonable to capture too much signal from the data during the construction of the Fréchet trees. So shallower trees are often used to avoid overfitting for RFWLLFR. Figure 5 shows the effect of the depth of Fréchet trees on the performance of our two methods based on setting I-2 with  $p = 10$  and  $n = 500$ . RFWLLFR achieves the optimal performance when the depth is six, while RFWLCFR prefers deeper Fréchet trees.

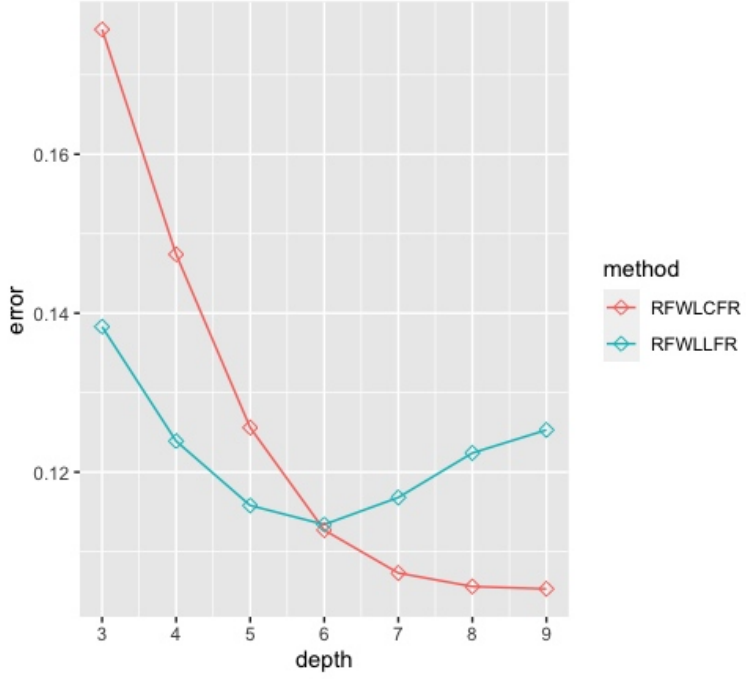


Figure 5: The influence of depth of Fréchet trees on average MSE for (10,500) from setting I-2.

We also select several combinations of  $(n, p)$  from setting I-2 to study the effect of noise size  $\sigma$  on the performance of each method. The results are summarized in Table 4. It can be seen that GFR is almost unaffected by noise. LFR performs poorly when the noise level is high. And our proposed RFWLCFR and RFWLLFR are still better than GFR and LFR in general.

Table 4: Average MSE (standard deviation) of different methods for  $(2, 200)$ ,  $(5, 500)$ ,  $(10, 1000)$ ,  $(20, 2000)$  from setting I-2 with different  $\sigma$  for 100 simulation runs

$(p, n)$	$\sigma$	GFR	LFR	RFWLCFR/FRF	RFWLLFR
$(2, 200)$	$\sigma = 0.1$	0.3026 (0.0283)	0.0261 (0.0198)	0.0158 (0.0036)	0.0084 (0.0041)
	$\sigma = 0.2$	0.3023 (0.0278)	0.0745 (0.1550)	0.0254 (0.0050)	0.0186 (0.0073)
	$\sigma = 0.5$	0.3032 (0.0274)	0.3341 (0.3412)	0.0895 (0.0181)	0.0786 (0.0209)
$(5, 500)$	$\sigma = 0.1$	0.2331 (0.0240)	NA	0.0515 (0.0080)	0.0437 (0.0074)
	$\sigma = 0.2$	0.2335 (0.0241)	NA	0.0557 (0.0087)	0.0502 (0.0083)
	$\sigma = 0.5$	0.2363 (0.0245)	NA	0.0850 (0.0128)	0.0946 (0.0144)
$(10, 1000)$	$\sigma = 0.1$	0.2434 (0.0295)	NA	0.0870 (0.0175)	0.0879 (0.0145)
	$\sigma = 0.2$	0.2438 (0.0297)	NA	0.0901 (0.0174)	0.0927 (0.0148)
	$\sigma = 0.5$	0.2462 (0.0302)	NA	0.1103 (0.0195)	0.1251 (0.0171)
$(20, 2000)$	$\sigma = 0.1$	0.2452 (0.0285)	NA	0.1227 (0.0225)	0.1300 (0.0191)
	$\sigma = 0.2$	0.2456 (0.0286)	NA	0.1257 (0.0238)	0.1337 (0.0194)
	$\sigma = 0.5$	0.2479 (0.0288)	NA	0.1401 (0.0260)	0.1654 (0.0235)

Since the components of the predictor  $X$  are independent in all previous simulation settings, we here add another setting to cover the case that components are correlated.

Setting I-3: We generate  $X$  by a multivariate normal distribution

$$X \sim \mathcal{N}(0, \Sigma),$$

where the  $ij$ -th element of  $\Sigma$  is  $0.5^{|i-j|}$ . Then  $Y$  is generated by

$$Y = \mathcal{N}(\mu_Y, \sigma_Y^2),$$

where

$$\mu_Y \sim \mathcal{N} (0.1(e_1^T X)^2 (2\beta^T X - 1), 0.2^2) \quad \text{and} \quad \sigma_Y = 1.$$

The above  $e_i$  is a vector of zeroes with 1 in the  $i$ th element. Consider the following four kinds of dimensions

- (i) For  $p = 2$ :  $\beta = (0.75, 0.25)$ .
- (ii) For  $p = 5, 10$ :  $\beta = (0.1, 0.2, 0.3, 0.4, 0, \dots, 0)$ .
- (iii) For  $p = 20$ :  $\beta = (0.1, 0.2, 0.3, 0.4, 0, \dots, 0, 0.1, 0.2, 0.3, 0.4) / 2$ .

Table 5: Average MSE (standard deviation) of different methods for setting I-3 for 100 simulation runs

Model	$(p, n)$	GFR	LFR	RFWLCFR/FRF	RFWLLFR
I-3	(2, 100)	0.2495 (0.2002)	0.0869 (0.3530)	0.1179 (0.1745)	0.0423 (0.0551)
	(2, 200)	0.2302 (0.3131)	0.0390 (0.1558)	0.0944 (0.2843)	0.0347 (0.1355)
	(5, 200)	0.0893 (0.0641)	NA	0.0429 (0.0432)	0.0342 (0.0261)
	(5, 500)	0.0827 (0.0551)	NA	0.0248 (0.0272)	0.0164 (0.0107)
	(10, 500)	0.0896 (0.1006)	NA	0.0368 (0.0660)	0.0307 (0.0293)
	(10, 1000)	0.0810 (0.0888)	NA	0.0226 (0.0623)	0.0187 (0.0201)
	(20, 1000)	0.0445 (0.0197)	NA	0.0181 (0.0119)	0.0210 (0.0085)
	(20, 2000)	0.0502 (0.0275)	NA	0.0155 (0.0110)	0.0172 (0.0081)

From the results in Table 5, we can find that the performance of GFR can not be improved significantly by simply increasing the number of training samples, but it performs better when the number of effective variables increases. RFWLLFR is the most stable among all methods. As the dimension of  $X$  becomes larger, the performance of RFWLCFR gets closer to that of RFWLLFR. Especially in the high-dimensional case, RFWLCFR begins to outperform RFWLLFR. Overall, all methods under the current setting behave similarly to the cases when the components of  $X$  are independent.

## B.2 Fréchet Regression for Symmetric Positive-definite Matrices

For responses being symmetric positive definite matrices, the intrinsic local polynomial regression (ILPR) (Yuan et al., 2012) and the manifold additive model (MAM) (Lin et al., 2022) are two promising tools which take advantage of the geometric structure of the Riemannian manifold. We plan to include the two methods for comparisons for Fréchet regression with symmetric positive-definite matrices.

The abelian group structure inherited from either the Log-Cholesky metric or the Log-Euclidean metric framework can turn the space of symmetric positive-definite matrices into a Riemannian manifold and further a bi-invariant Lie group. Lin et al. (2022) further proposed an additive model for the regression of symmetric positive-definite matrices valued response and an effective method called the manifold additive model (MAM). Their numerical studies show that the proposed method enjoys superior numerical performance compared with the intrinsic local polynomial regression (ILPR, Yuan et al. (2012)), especially when the underlying model is fully additive. However, Lin et al. (2022) only considered  $p = 3, 4$  in their simulation studies. In the next, we adopt the settings in Lin et al. (2022) to make a comprehensive comparisons among MAM, ILPR, GFR, FRF, RFWLCFR, and RFWLLFR. MAM can be implemented with the R-package ‘‘matrix-manifold’’ (Lin, 2020).

Setting II: Let  $X \sim \mathcal{U}([0, 1]^p)$ . The response  $Y$  is generated via

$$Y = \mu \oplus w(X) \oplus \zeta,$$

where  $\mu$  is the  $3 \times 3$  identity matrix,  $w(X) = \exp_{\mu, e} f(X)$ ,  $e$  is the identity element of the group,  $\exp_{\mu, e}$  denotes the parallel transport from  $\mu$  to  $e$ ,  $\exp(\cdot)$  denotes the Lie exponential map,  $\oplus$  denotes the group operation, and  $\zeta$  is the random noise. The noise  $\zeta$  is generated according to  $\log \zeta = \sum_{j=1}^6 Z_j v_j$ , where  $\log(\cdot)$  denotes the Lie log map,  $Z_1, \dots, Z_6$  are independently sampled from  $\mathcal{N}(0, \sigma^2)$ , and  $v_1, \dots, v_6$  are an orthonormal basis of the tangent space  $T_e \mathcal{S}_3^+$ . The signal-to-ratio (SNR) is measured by  $\text{SNR} = E \|\log w(X)\|_e^2 / E \|\log \zeta\|_e^2$ . Take the value of the parameter  $\sigma^2$  to cover two choices for the SNR, namely,  $\text{SNR} = 2$  and  $\text{SNR} = 4$ . Refer to Lin et al. (2022) for the details of the notations and concepts here. We consider the following setting about  $f(X)$ .

II-3:  $f(X) = \sum_{k=1}^q f_k(x_k)$  with  $f_k(x_k)$  being an  $3 \times 3$  matrix whose  $(j, l)$ -entry is  $g(x_k; j, l, q) = \exp(-|j - l|/q) \sin(2q\pi \{x_k - (j + l)/q\})$ .

II-4:  $f(X) = f_{12}(x_1, x_2) \prod_{k=3}^q f_k(x_k)$ , where  $f_{12}(x_1, x_2)$  is an  $3 \times 3$  matrix whose  $(j, l)$ -entry is  $\exp\{-(j + l)(x_1 + x_2)\}$ , and  $f_k(x_k)$  is an  $3 \times 3$  matrix whose  $(j, l)$ -entry is  $\sin(2\pi x_k)$ .

To maintain the consistency of the simulations, we use the same way as Lin et al. (2022) to measure the quality of the estimation. For settings II-3 and II-4, we consider  $p = 3, 4, 10, 20$  and two choices of  $n$  for each  $p$ . For  $p = 3, 4$ , the setting is the same as Lin et al. (2022). For  $p = 10, 20$ , we increase the dimension of  $X$ , but  $Y$  is still only related

to the first four components of  $X$ , *i.e.*,  $q = 4$ . Table 6 shows the results. For the setting II-3 where the underlying model is additive, MAM shows clear advantages when  $p$  is relatively small. Although the three methods based on Fréchet trees are not optimal, they are significantly better compared to ILPR. For non-additive setting II-4, RFWLCFR/FRF tends to perform the best. This setting also indicates that there are indeed cases where RFWLLFR will perform worse than RFWLCFR. It may be more efficient for complex settings to use RFWLCFR, whose mechanism is similar to that of random forests. Since both MAM and GFR make specific model assumptions, setting II-4 is not suitable for these two methods, although MAM performs slightly better than GFR. In particular, when  $p$  is greater than 10, the implementations of MAM and ILPR often fail to work, and they are not feasible when the dimension of  $X$  is too large. Through this experiment, we again demonstrate the outstanding performance of our method in the field of high-dimensional non-parametric Fréchet regression. In real applications, we often lack prior knowledge of the structure of the underlying model, so it is important to develop regression methods that suit all situations with excellent performance.

Table 6: Average MSE (standard deviation) of different methods for setting II-3,4 with SNR= 2, 4 and Log-Cholesky metric for 100 simulation runs

Model	( $p, n$ )	MAM	ILPR	GFR	RFWLCFR/FRF	RFWLLFR
II-3 (SNR= 2)	(3, 100)	0.415 (0.023)	0.922 (0.126)	0.970 (0.012)	0.714 (0.018)	0.794 (0.023)
	(3, 200)	0.299 (0.017)	0.796 (0.064)	0.956 (0.008)	0.613 (0.013)	0.655 (0.017)
	(4, 100)	0.527 (0.028)	0.965 (0.033)	0.986 (0.013)	0.805 (0.018)	0.923 (0.029)
	(4, 200)	0.357 (0.019)	0.916 (0.021)	0.970 (0.010)	0.748 (0.014)	0.832 (0.018)
	(10, 500)	NA	NA	0.967 (0.008)	0.774 (0.014)	0.929 (0.015)
	(10, 1000)	NA	NA	0.959 (0.009)	0.742 (0.012)	0.879 (0.011)
	(20, 1000)	NA	NA	0.966 (0.009)	0.778 (0.011)	0.956 (0.014)
	(20, 2000)	NA	NA	0.958 (0.008)	0.752 (0.010)	0.917 (0.012)
II-4 (SNR= 2)	(3, 100)	0.744 (0.054)	0.672 (0.189)	0.773 (0.051)	0.501 (0.051)	0.540 (0.058)
	(3, 200)	0.713 (0.049)	0.481 (0.087)	0.761 (0.049)	0.439 (0.037)	0.465 (0.041)
	(4, 100)	0.841 (0.065)	0.834 (0.146)	0.855 (0.064)	0.676 (0.078)	0.788 (0.125)
	(4, 200)	0.835 (0.063)	0.758 (0.113)	0.841 (0.060)	0.601 (0.073)	0.684 (0.092)
	(10, 500)	NA	NA	0.838 (0.061)	0.681 (0.076)	0.773 (0.068)
	(10, 1000)	NA	NA	0.829 (0.061)	0.643 (0.077)	0.718 (0.070)
	(20, 1000)	NA	NA	0.836 (0.061)	0.736 (0.079)	0.838 (0.074)
	(20, 2000)	NA	NA	0.830 (0.060)	0.698 (0.078)	0.783 (0.072)
II-3 (SNR= 4)	(3, 100)	0.346 (0.022)	0.916 (0.136)	0.965 (0.011)	0.693 (0.017)	0.755 (0.019)
	(3, 200)	0.229 (0.011)	0.774 (0.058)	0.954 (0.008)	0.589 (0.012)	0.616 (0.015)
	(4, 100)	0.449 (0.033)	0.948 (0.030)	0.979 (0.012)	0.789 (0.017)	0.884 (0.025)
	(4, 200)	0.284 (0.012)	0.902 (0.026)	0.966 (0.010)	0.734 (0.013)	0.802 (0.016)
	(10, 500)	NA	NA	0.964 (0.008)	0.764 (0.013)	0.894 (0.013)
	(10, 1000)	NA	NA	0.958 (0.009)	0.732 (0.012)	0.847 (0.011)
	(20, 1000)	NA	NA	0.964 (0.009)	0.771 (0.010)	0.919 (0.013)
	(20, 2000)	NA	NA	0.957 (0.008)	0.744 (0.010)	0.886 (0.011)
II-4 (SNR= 4)	(3, 100)	0.736 (0.054)	0.655 (0.199)	0.770 (0.051)	0.466 (0.054)	0.477 (0.059)
	(3, 200)	0.709 (0.049)	0.439 (0.084)	0.760 (0.048)	0.404 (0.040)	0.401 (0.043)
	(4, 100)	0.841 (0.066)	0.853 (0.162)	0.851 (0.066)	0.656 (0.083)	0.746 (0.126)
	(4, 200)	0.834 (0.063)	0.758 (0.131)	0.839 (0.060)	0.582 (0.076)	0.648 (0.093)
	(10, 500)	NA	NA	0.836 (0.061)	0.675 (0.076)	0.749 (0.069)
	(10, 1000)	NA	NA	0.829 (0.061)	0.636 (0.080)	0.696 (0.074)
	(20, 1000)	NA	NA	0.835 (0.061)	0.734 (0.080)	0.822 (0.078)
	(20, 2000)	NA	NA	0.830 (0.060)	0.695 (0.076)	0.769 (0.070)

### B.3 Fréchet regression for spherical data

The estimation errors of setting III-1,2 are recorded in Table 7.

Table 7: Average MSE (standard deviation) of different methods for setting III-1,2 with  $\sigma = 0.2$  for 100 simulation runs

Model	$(p, n)$	FRF	RFWLCFR	RFWLLFR
III-1	(2, 100)	0.032329 (0.007413)	0.032327 (0.007409)	0.019839 (0.005842)
	(2, 200)	0.023078 (0.003967)	0.023079 (0.003967)	0.010781 (0.002704)
	(5, 200)	0.030237 (0.004693)	0.030237 (0.004693)	0.017935 (0.003892)
	(5, 500)	0.021684 (0.002725)	0.021683 (0.002724)	0.012164 (0.001998)
	(10, 500)	0.035012 (0.004252)	0.035018 (0.004253)	0.013339 (0.001915)
	(10, 1000)	0.027184 (0.003063)	0.027188 (0.003065)	0.010851 (0.001389)
	(20, 1000)	0.034698 (0.003879)	0.034701 (0.003879)	0.033069 (0.004379)
	(20, 2000)	0.029362 (0.003503)	0.029362 (0.003502)	0.028837 (0.003453)
III-2	(2, 100)	0.010498 (0.002954)	0.010501 (0.002954)	0.004226 (0.001735)
	(2, 200)	0.007982 (0.001836)	0.007984 (0.001837)	0.003150 (0.000956)
	(5, 200)	0.008893 (0.001612)	0.008894 (0.001612)	0.005192 (0.001418)
	(5, 500)	0.006562 (0.001216)	0.006563 (0.001216)	0.002946 (0.000637)
	(10, 500)	0.008936 (0.001378)	0.008938 (0.001378)	0.005266 (0.000962)
	(10, 1000)	0.007110 (0.000951)	0.007111 (0.000952)	0.004190 (0.000626)
	(20, 1000)	0.009005 (0.001258)	0.009006 (0.001259)	0.006311 (0.000975)
	(20, 2000)	0.007427 (0.000938)	0.007429 (0.000938)	0.005117 (0.000692)

## C Asymptotic Normality of the $M_{m_n}$ -estimator

We first generalize the theory of  $M_m$ -estimator in [Bose and Chatterjee \(2018\)](#) to the case that  $m$  tends to infinity along with  $n$ .

**Definition 1.** Let  $Z_1, Z_2, \dots, Z_{m_n}$  be i.i.d.  $\mathcal{Z}$ -valued random variables and  $\theta \in \mathcal{R}^d$ . Let  $f_n(z_1, z_2, \dots, z_{m_n}, \theta)$  be a real valued measurable function which is symmetric in the arguments  $z_1, z_2, \dots, z_{m_n}$  for each  $n$ . Define

$$Q_n(\theta) = E f_n(Z_1, Z_2, \dots, Z_{m_n}, \theta)$$

and

$$\theta_n = \underset{\theta \in \mathcal{R}^d}{\operatorname{argmin}} Q_n(\theta).$$

$\theta_n$  is called the  $M_{m_n}$ -parameter.

**Definition 2.** Let  $Z_1, Z_2, \dots, Z_n$  be a sequence of i.i.d. observations. Define

$$\hat{Q}_n(\theta) = \binom{n}{m_n}^{-1} \sum_{1 \leq i_1 < i_2 < \dots < i_{m_n} \leq n} f_n(Z_{i_1}, Z_{i_2}, \dots, Z_{i_{m_n}}, \theta)$$

and

$$\hat{\theta}_n = \underset{\theta \in \mathcal{R}^d}{\operatorname{argmin}} \hat{Q}_n(\theta).$$

$\hat{\theta}_n$  is called the  $M_{m_n}$ -estimator of  $\theta_n$ .

In the above definition, a hidden assumption is  $m_n/n \rightarrow 0$ . Actually,  $\hat{Q}_n(\theta)$  is an infinite order U-process about  $\theta$ . Since  $\hat{Q}_n(\theta)$  is the sample analogue of  $Q_n(\theta)$ ,  $\hat{\theta}_n$  is a reasonable estimator of  $\theta_n$ . When  $m_n = 1$ ,  $\hat{\theta}_n$  is the classical M-estimator. When  $m_n = m$  is a fixed positive integer,  $\hat{\theta}_n$  is the  $M_n$ -estimator studied in [Bose and Chatterjee \(2018\)](#). By an appropriate selection theorem, it is often possible to choose a measurable version of  $\hat{\theta}_n$ . We always work with such a version. Please refer to section 2.3 of [Bose and Chatterjee \(2018\)](#) for more details.

Let  $g_n$  be a measurable sub-gradient of  $f_n(z_1, z_2, \dots, z_{m_n}, \theta)$  about  $\theta$ . Define

$$K_n = \operatorname{Var} [E \{g_n(Z_1, Z_2, \dots, Z_{m_n}, \theta_n) \mid Z_1\}],$$

$$U_n = \binom{n}{m_n}^{-1} \sum_{1 \leq i_1 < i_2 < \dots < i_{m_n} \leq n} g_n(Z_{i_1}, Z_{i_2}, \dots, Z_{i_{m_n}}, \theta_n).$$

In order to achieve the asymptotic normality of the  $M_{m_n}$ -estimator, we need the following assumptions.

(i)  $f_n(z_1, z_2, \dots, z_{m_n}, \theta)$  is measurable in  $(z_1, z_2, \dots, z_{m_n})$  and convex in  $\theta$  for each  $n$ .

- (ii)  $Q_n(\theta)$  is finite for each  $\theta$  and  $n$ .
- (iii)  $\theta_n$  exists and is unique for each  $n$ , and  $f_n(z_1, z_2, \dots, z_{m_n}, \theta)$  is twice differentiable on an appropriate neighborhood of  $\theta_n$ .
- (iv)  $E|g_n(Z_1, Z_2, \dots, Z_{m_n}, \theta_n)|^2 < \infty$  for each  $n$ , and  $m_n \lambda_{\min}(K_n) \not\rightarrow 0$ , where  $\lambda_{\min}(K_n)$  denotes the smallest eigenvalue of  $K_n$ .
- (v)  $H_n = \nabla^2 Q(\theta_n)$  exists and is positive definite for each  $n$  and  $\lambda_{\min}(H_n) \not\rightarrow 0$ .

Through the definition, we know that the  $M_{m_n}$ -estimator is an implicit solution to the infinite order U-process. Under the above assumptions, we can derive  $\hat{\theta}_n$  a weak representation through the linearization of the infinite order U-statistic  $U_n$ . Therefore, the asymptotic normality of infinite order U-statistics determines the asymptotic normality of the  $M_{m_n}$ -estimator  $\hat{\theta}_n$ . [Mentch and Hooker \(2016\)](#) gave sufficient conditions for asymptotic normality of such U-statistics. However, these conditions can not hold simultaneously. [DiCiccio and Romano \(2020\)](#) then developed conditions which can be verified on the basis of [Mentch and Hooker \(2016\)](#). But both of their results require that the order of the infinite order U-statistics is  $o(n^{1/2})$ . [Peng et al. \(2019\)](#) further improved this result when the order of the infinite order U-statistics is  $o(n)$ . [Wager and Athey \(2018\)](#) also gave the same rate (ignoring the log-factors) when focusing on random forests with some additional requirements on the construction of trees. Our assumption (iv) here is to ensure the asymptotic normality of  $U_n$  by the result of [Peng et al. \(2019\)](#). And assumptions (i), (ii), (iii) and (v) are adaptions of that for studying  $M_m$  estimator in [Bose and Chatterjee \(2018\)](#).

**Theorem 6.** Suppose that assumptions (i)-(v) hold, then for any sequence of measurable minimizers  $\{\hat{\theta}_n, n \geq 1\}$ ,

- (a)  $\hat{\theta}_n - \theta_n = -H_n^{-1}U_n + o_p\left(\left(\frac{m_n}{n}\right)^{1/2}\right)$ ,
- (b)  $n^{1/2}\Lambda_n^{-1/2}(\hat{\theta}_n - \theta_n) \xrightarrow{d} \mathcal{N}(0, I)$ , where

$$\Lambda_n = m_n^2 H_n^{-1} K_n H_n^{-1}.$$

Theorem 6 establishes the asymptotic normality of  $M_{m_n}$ -estimator, which is a generalization of the central limit theorem of the  $M_m$ -estimator given in [Bose and Chatterjee \(2018\)](#).

## References

Arlot, S. and Genuer, R. (2014). Analysis of purely random forests bias. *arXiv preprint arXiv:1407.3939*.

Athey, S., Tibshirani, J., and Wager, S. (2019). Generalized random forests. *The Annals of Statistics*, 47(2):1148–1178.

Bhattacharjee, S. and Müller, H.-G. (2021). Single index fréchet regression. *arXiv preprint arXiv:2108.05437*.

Bhattacharya, R. and Lin, L. (2017). Omnibus clts for fréchet means and nonparametric inference on non-euclidean spaces. *Proceedings of the American Mathematical Society*, 145(1):413–428.

Bhattacharya, R. and Patrangenaru, V. (2003). Large sample theory of intrinsic and extrinsic sample means on manifolds. *The Annals of Statistics*, 31(1):1–29.

Bhattacharya, R. and Patrangenaru, V. (2005). Large sample theory of intrinsic and extrinsic sample means on manifolds: II. *Annals of statistics*, pages 1225–1259.

Biau, G. (2012). Analysis of a random forests model. *Journal of Machine Learning Research*, 13:1063–1095.

Biau, G., Devroye, L., and Lugosi, G. (2008). Consistency of random forests and other averaging classifiers. *Journal of Machine Learning Research*, 9(9).

Bloniarz, A., Talwalkar, A., Yu, B., and Wu, C. (2016). Supervised neighborhoods for distributed nonparametric regression. In *Artificial Intelligence and Statistics*, pages 1450–1459. PMLR.

Bose, A. and Chatterjee, S. (2018). *U-statistics, Mm-estimators and Resampling*. Springer.

Breiman, L. (2001). Random forests. *Machine learning*, 45(1):5–32.

Capitaine, L. (2021). Frechforest: Frechet random forests. *R package version 0.95*.

Capitaine, L., Bigot, J., Thiébaut, R., and Genuer, R. (2019). Fréchet random forests for metric space valued regression with non euclidean predictors. *arXiv preprint arXiv:1906.01741*.

Chen, Y., Gajardo, A., Fan, J., Zhong, Q., Dubey, P., Han, K., Bhattacharjee, S., and Müller, H.-G. (2020). frechet: Statistical analysis for random objects and non-euclidean data. *R package version 0.2.0*.

Chen, Y. and Müller, H.-G. (2022). Uniform convergence of local fréchet regression with applications to locating extrema and time warping for metric space valued trajectories. *The Annals of Statistics*, 50(3):1573–1592.

Denil, M., Matheson, D., and Freitas, N. (2013). Consistency of online random forests. In *International conference on machine learning*, pages 1256–1264. PMLR.

DiCiccio, C. and Romano, J. P. (2020). Clt for u-statistics with growing dimension. Technical report, Technical report, Standford University.

Duroux, R. and Scornet, E. (2018). Impact of subsampling and tree depth on random forests. *ESAIM: Probability and Statistics*, 22:96–128.

Friedberg, R., Tibshirani, J., Athey, S., and Wager, S. (2020). Local linear forests. *Journal of Computational and Graphical Statistics*, pages 1–15.

Gao, W. and Zhou, Z.-H. (2020). Towards convergence rate analysis of random forests for classification. *Advances in Neural Information Processing Systems*, 33.

Genuer, R. (2012). Variance reduction in purely random forests. *Journal of Nonparametric Statistics*, 24(3):543–562.

Heilig, C. and Nolan, D. (2001). Limit theorems for the infinite-degree u-process. *Statistica Sinica*, pages 289–302.

Heilig, C. M. (1997). *An empirical process approach to U-processes of increasing degree*. University of California, Berkeley.

Hein, M. (2009). Robust nonparametric regression with metric-space valued output. In *Advances in Neural Information Processing Systems*, pages 718–726. Citeseer.

Jeon, J. M., Lee, Y. K., Mammen, E., and Park, B. U. (2022). Locally polynomial hilbertian additive regression. *Bernoulli*, 28(3):2034–2066.

Jeon, J. M. and Park, B. U. (2020). Additive regression with hilbertian responses. *The Annals of Statistics*, 48(5):2671–2697.

Klusowski, J. (2021). Sharp analysis of a simple model for random forests. In *International Conference on Artificial Intelligence and Statistics*, pages 757–765. PMLR.

Lin, Y. and Jeon, Y. (2006). Random forests and adaptive nearest neighbors. *Journal of the American Statistical Association*, 101(474):578–590.

Lin, Z. (2019). Riemannian geometry of symmetric positive definite matrices via cholesky decomposition. *SIAM Journal on Matrix Analysis and Applications*, 40(4):1353–1370.

Lin, Z. (2020). matrix-manifold: Basic operations and functions on matrix manifolds. *R package version 0.1.0*.

Lin, Z., Müller, H., and Park, B. (2022). Additive models for symmetric positive-definite matrices and lie groups. *Biometrika*.

Meinshausen, N. and Ridgeway, G. (2006). Quantile regression forests. *Journal of Machine Learning Research*, 7(6).

Mentch, L. and Hooker, G. (2016). Quantifying uncertainty in random forests via confidence intervals and hypothesis tests. *Journal of Machine Learning Research*, 17(1):841–881.

Moakher, M. (2005). A differential geometric approach to the geometric mean of symmetric positive-definite matrices. *SIAM Journal on Matrix Analysis and Applications*, 26(3):735–747.

Peng, W., Coleman, T., and Mentch, L. (2019). Asymptotic distributions and rates of convergence for random forests via generalized u-statistics. *arXiv preprint arXiv:1905.10651*.

Pennec, X., Fillard, P., and Ayache, N. (2006). A riemannian framework for tensor computing. *International Journal of computer vision*, 66(1):41–66.

Petersen, A. and Müller, H.-G. (2019). Fréchet regression for random objects with euclidean predictors. *The Annals of Statistics*, 47(2):691–719.

Scornet, E., Biau, G., and Vert, J.-P. (2015). Consistency of random forests. *The Annals of Statistics*, 43(4):1716–1741.

van der Vaart, A. and Wellner, J. A. (1996). *Weak convergence and empirical processes: with applications to statistics*. Springer Science & Business Media.

Wager, S. and Athey, S. (2018). Estimation and inference of heterogeneous treatment effects using random forests. *Journal of the American Statistical Association*, 113(523):1228–1242.

Ying, C. and Yu, Z. (2022). Fréchet sufficient dimension reduction for random objects. *Biometrika*, 109(4):975–992.

Yuan, Y., Zhu, H., Lin, W., and Marron, J. S. (2012). Local polynomial regression for symmetric positive definite matrices. *Journal of the Royal Statistical Society: Series B (Statistical Methodology)*, 74(4):697–719.

Zhang, Q., Xue, L., and Li, B. (2021). Dimension reduction and data visualization for fréchet regression. *arXiv preprint arXiv:2110.00467*.